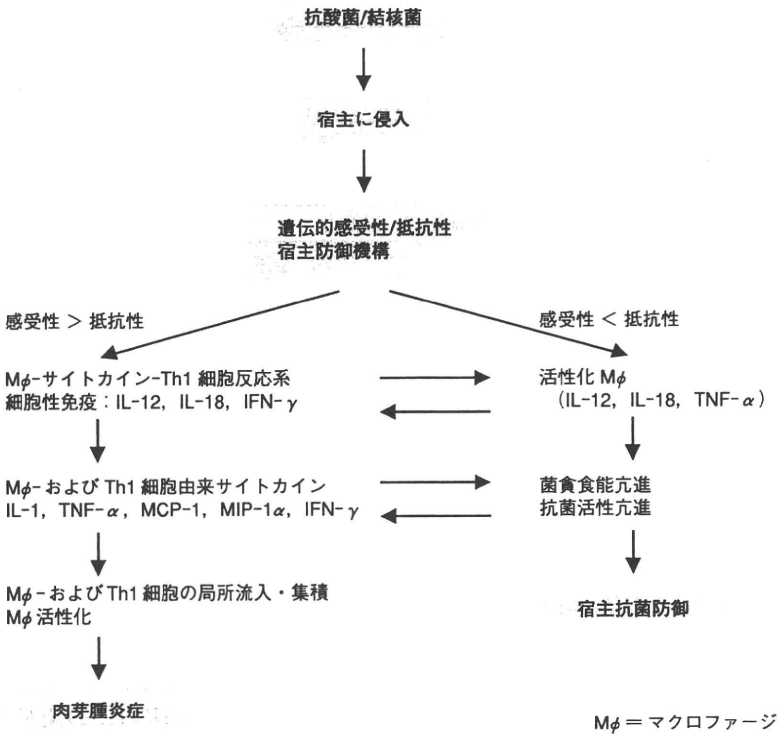

図 IV-55　抗酸菌/結核菌感染における宿主細胞および機能分子応答機構

パ節の石灰化瘢痕を形成する(**初期変化群**：Ghon complex)。

2) 二次結核と播種性結核

宿主が結核菌に既感染し，免疫学的感作が成立している場合，すなわち外来性再感染，内因性再燃，一次感染病巣から直接，全身播種性結核に進展した場合などがある。これらの誘因には結核菌の高病原性や宿主の易感染性が関与している。二次結核における肉芽腫形成部位は肺尖部に最も多くみられるが，他部位の肺，腎臓，髄膜や骨髄などにも播種する。これらの肉芽腫病変は結核における組織傷害の主因であり，その機序には遅延型過敏反応が寄与している。二次結核に特徴的所見は**乾酪壊死**と**空洞形成**であり，これらの病変から結核菌が血行を介して全身に撒布，また，気道を介して排泄され，感染源(飛沫核感染)となる。

a 結核 tuberculosis

結核は再興感染症の代表であり，1993 年に世界保健機関(WHO)，1999 年に厚生省(現厚生労働省)が「結核緊急事態宣言」を発表，結核問題を再認識し，結核制圧対策の強化に取り組んでいくことを提言している。また，2000 年沖縄で開催された G8 サミットは結核，エイズとマラリアによる年間発生患者数が 3 億人，死亡数が 500 万人以上であることから，これら 3 感染症を人類の健康被害における重点疾患(世界三大感染症)と認識し，協調して介入していくことを決議している。結核対策は，① 感染源対策(感染性の高い患者の早期発見・診断，隔離や確実な治療)，② 感染経路対策(個室収容，独立空調，マスクの着用)，③ 感受性宿主対策(ワクチン接種や抗結核薬による化学予防)および，④ 一般国民や医療従事者への啓発・教育から構成される。

結核対策の目標として WHO は，① 2005 年までに 70% 以上の感染性(喀痰塗抹陽性)結核患者の発見と 85% 以上の治癒，② 2010 年までに結核死亡や有病率を 2001 年の統計に比べて 50% 以下にすること，③ 2050 年までに結核を世界的な公衆衛生問題からなくすことを目標設定している。

1) 発生動向

全世界では約 20 億人(全人口の 1/3)が結核菌

表 IV-55　結核菌の特徴

細胞内寄生性	桿菌(0.2〜0.6×1〜10 μm)，宿主細胞，特に，マクロファージ内で抗菌機構から逃れて増殖
細胞壁	脂質成分が豊富なため，疎水性であり，化学物質にも安定，グラム染色に難染色性，抗酸性
好気性	酸素分圧の高い臓器(肺など)で増殖し，病変を形成
遅発育性	至適温度：37℃，倍加時間：約 12〜15 時間，培養集落形成に 4〜8 週間
感染形式	飛沫核/空気感染
病原性	慢性炎症，肉芽腫，乾酪壊死，空洞形成，線維化
遺伝子	全ゲノム(約 4.41 Mb)の解読

Mycobacterium tuberculosis に既感染しており，毎年 920 万人が結核を発病，170 万人(HIV/エイズ合併を含む)が死亡し，有病者は 2,200 万人であるといわれている。今後 10 年間，少なくとも，8,000 万人が発病，2,000 万人が死亡することが推定されている。わが国では，年間 25,300 人(罹患率人口 10 万対：19.8)が結核を発病し，2,200 人(死亡率：1.7)が死亡しており，有病者は 21,000 人(有病率：16.2)と報告されている(2007 年)。

結核は単一病原体による感染症として，世界最大である。疫学的に懸念される事項として，① 急速な人口の高齢化に伴う高齢者結核の増加(70 歳以上の占める割合：約 47%)，② 国内地域格差の拡大，③ 多剤耐性結核菌の出現(初回耐性：1%，獲得耐性：20%)，④ ヒト免疫不全ウイルス感染症(エイズを含む)の重複感染などがある。

2) 病原体

結核菌の生物学的特徴(表 IV-55)として，① 細胞内寄生性，② 脂質成分に富む細胞壁，③ 好気性，④ 遅発育性，⑤ 飛沫核(空気)感染，⑥ 慢性炎症，⑦ 遺伝子の解読などがある。結核菌は好気性グラム陽性桿菌，細胞内寄生病原体であるが，細胞壁が長炭素鎖脂肪酸(ミコール酸)に富み，グラム染色では**難染色性**を示す。そのため，抗酸性(**チール・ネールゼン** Ziehl-Neelsen，キニヨン Kinyoun)染色や蛍光染色が用いられる。抗酸性染色は石炭酸フクシンで加温染色後，塩酸アルコールで脱色，メチレンブルーで後染色する。抗酸菌は“赤い桿菌”として観察される。抗酸菌以外の通常細菌やヒト組織・細胞は後染色のメチレンブルーにより“青く”対比染色される。抗酸菌をオーラミンやローダミンなどの蛍光色素を用いて染色し，塩酸アルコールで脱色後，蛍光顕微鏡で観察する蛍光染色法も広く用いられている。蛍光顕微鏡で観察すると，暗い背景下に抗酸菌は“緑青-橙-黄色”の蛍光を発する。分裂倍加時間は約 12〜15 時間の遅発育菌であり，感染伝播は飛沫核(空気)感染による。宿主防御機構では，マクロファージ-サイトカイン-T 細胞応答系，すなわち，細胞性免疫が役割を演じ，細胞内殺菌物質として，ガス状物質(反応性酸素化合物質や反応性窒素化合物質)が寄与している。その結果，結核菌感染者の約 10% が一生涯において結核を発病する。病変は慢性炎症，肉芽腫，乾酪壊死，空洞形成や線維化などが特徴的である。

M. tuberculosis H37Rv の全ゲノム塩基配列が解明された。今後，遺伝子解析を基盤とした科学的戦略が推進され，分子・遺伝子標的を視点とした新規診断法，抗結核薬の開発，薬剤耐性獲得機構の解明や新規ワクチン開発が展開されるであろう。

3) 臨床症状

結核は肺結核と肺外結核に分類されるが，80% 以上は肺結核である。肺結核の症状として，咳嗽や喀痰(持続性，2 週間以上)，血痰，胸痛，軽度発熱，体重減少があるが，特に，持続性咳嗽と喀痰は重要である。肺外結核部位として，リンパ節，胸膜，泌尿生殖器，骨・関節，髄膜・中枢神経系，腹膜・消化管や心外膜などがある(表 IV-56)。

4) 診断

診断には，病原体および補助診断がある(表 IV-57)。病原体診断は確定的であるが，塗抹検査陽性(図 IV-56，294 頁)の場合，結核菌のみならず，非結核性抗酸菌を考慮する必要がある(後述)。現在，最も信頼性の高い検査は培養法(図 IV-57，294 頁)であるが，長期間を要することが欠点である(固形培地：4〜8 週間，液体培地：10〜14 日間)。PCR(図 IV-58，294 頁)などの核酸増幅法は迅速性，感度や特異性に優れるが，生死菌の識別や技術的問題(熟練，偽陽性・偽陰性)がある。

表 IV-56　肺外結核の所見

病変部位	好発	臨床症状	診断	治療や管理
リンパ節	若年者-成人初期 女性＞男性	通常，片側性，疼痛はない	生検や培養	抗結核化学療法
胸膜	若年者-成人	胸水，乾性咳嗽	胸水単核細胞浸潤 胸水-結核菌塗抹検査：陰性が多い 胸膜生検および培養	抗結核化学療法
泌尿生殖器	若年者ではまれ 女性＞男性	腎臓，尿管，膀胱，精巣，精巣上体，子宮，卵管	尿培養，生検-培養，子宮内容掻爬物-培養	抗結核化学療法
骨・関節	全年齢にみられるが，高齢者に好発	高齢者：下部胸椎や腰椎 若年者：上部胸椎 関節可動域の制限や変形(亀背)	生検および培養	抗結核化学療法 罹患部切除 関節癒合の防止
髄膜/中枢神経系	乳幼児や小児	発熱，頭痛，倦怠感，意識障害，痙攣，昏睡	腰椎穿刺による脳脊髄液検査 塗抹や培養	抗結核化学療法 副腎皮質ステロイド療法
腹膜/消化管	成人や高齢者	腹部膨満や腹痛，Crohn病に類似	内視鏡による生検や培養	抗結核化学療法 副腎皮質ステロイド療法 癒着や閉塞に注意
播種性	幼年者や高齢者	発熱や衰弱	罹患臓器の塗抹や培養 ツベルクリン皮内反応：約半数が陰性 胸部 X 線異常所見：初期に欠き，遅れて出現	早期の抗結核化学療法 副腎皮質ステロイド療法の評価は未確定

表 IV-57　結核の診断

病原体診断	塗抹検査	抗酸菌染色(Ziehl-Neelsen，Kinyoun 染色)，蛍光染色
	培養検査	固形培地(卵培地：小川，Löwenstein-Jensen，寒天培地：Middlebrook 7H10，7H11)：4〜8 週間 液体培地(MGIT，MB check)：10〜14 日 薬剤感受性試験
	遺伝子検出	核酸増幅法：polymerase chain reaction(PCR) DNA-DNA ハイブリダイゼーション 薬剤耐性遺伝子
補助診断	胸部 X 線	中および上肺野病変(浸潤，結節や空洞) リンパ節腫大や石灰化 胸膜炎／胸水貯留
	病理学的検査	乾酪壊死を伴う肉芽腫
	TST	ツベルクリン皮内反応(Mantoux) 48 時間後判定：遅延型皮内反応(IV 型) 陽性：結核菌感染，BCG 陽転，非結核性抗酸菌感染 陰性：未感染，BCG 未接種，免疫不全(HIV/エイズ，重症結核，薬物性)
	IGRA：QFT	末梢血細胞 IFN-γ 産生・遊離試験(IGRA，Quantiferon)：*in vitro* 指標；IFN-γ 抗原；ツベルクリン蛋白質，RD1(ESAT-6，CFP-10)
全身播種性		血行性撒布(髄膜，網膜，肺，肝，腎臓)：小児，免疫不全

TST：tuberculin skin test，IGRA：interferon gamma release assay，QFT：Quantiferon

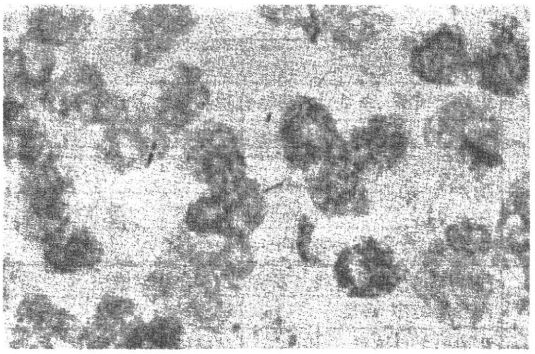

図Ⅳ-56　結核菌の喀痰塗抹検査(Ziehl-Neelsen 染色)
結核菌は赤染されている桿菌であり，ヒト組織は青染されている。

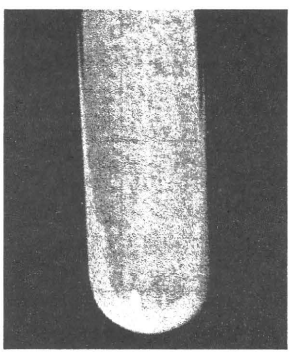

図Ⅳ-57　結核菌の培養所見
喀痰を卵(小川)培地に接種し，6週間後に多数の集落(乳白色～薄黄色)形成を認めた。

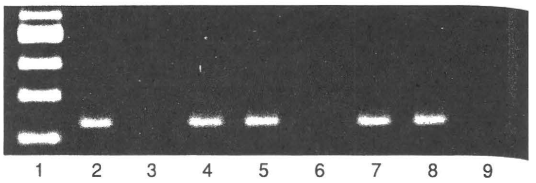

図Ⅳ-58　核酸増幅法による結核菌遺伝子の検出
結核菌 DNA に特異的なプライマーを用い，ポリメラーゼ連鎖反応で喀痰の結核菌遺伝子を検出した。
分子サイズマーカー：レーン1
陽性：レーン2，4，5，7，8
陰性：レーン3，6，9

図Ⅳ-59　肺結核の胸部X線所見
浸潤影，結節，線維化，肺門リンパ節腫大，胸膜肥厚・癒着や胸水貯留など，多彩な所見を認めた。

胸部X線所見では，浸潤影，結節，空洞，線維化，肺門リンパ節腫大や石灰化，無気肺，胸膜肥厚・癒着，胸水貯留など多彩である(図Ⅳ-59)。好発部位は肺尖を含む上肺や中肺野である。多発性びまん性結節陰影は播種(粟粒)性結核でみられる。これらの所見は他の炎症性や腫瘍性肺疾患にも認められる所見であり，結核特異的でなく，注意を要するため，結核の補助的診断法として用いられる。

ツベルクリン皮内反応 tuberculin skin test (TST)の陽性(わが国：紅斑長径≧10 mm，欧米：硬結長径≧5 mm)は結核菌感染のみならず，BCG 接種や非結核性抗酸菌感染でもみられ，逆に，活動性結核患者の約25%は陰性である。陰性は真の陰性(結核菌未感染)や偽陰性(結核菌既感染にもかかわらず陰性)を包含する。偽陰性として，栄養障害，高齢者，免疫疾患，リンパ系悪性腫瘍，副腎皮質ステロイド薬療法，慢性腎不全，サルコイドーシス，HIV 感染者(エイズを含む)や重症結核(播種性)などがある。したがって，ツベルクリン皮内反応は結核の補助的診断法である。また，ツベルクリン皮内反応陽性は感染防御の指標とならないことも留意する。

近年，結核菌特異的タンパク質抗原(ESAT-6 や CFP-10)を用いた免疫学的診断法が開発され，臨床応用されている(interferon-γ 遊離試験：IGRA，Quantiferon：QFT)。これらの抗原は BCG や多くの非結核性抗酸菌に存在しないため，結核菌感染を特異的に検出できる。原理は，末梢血に特異的タンパク質抗原を加え，培養後，産生・遊離される IFN-γ を定量する(陽性：0.35 IU/ml 以上)。検査対象として，① 潜在性結核菌感染や ② 活動性結核の補助診断に応用されている。

表 IV-58　代表的な抗結核薬の作用機序と副作用

薬剤	作用機序	主な副作用
イソニアジド(INH)	細胞壁ミコール酸合成阻害	末梢神経障害，肝障害 ビタミン B_6 にて予防可
リファンピシン(RIF)	DNA 依存性 RNA ポリメラーゼ阻害	血小板減少，赤色尿，アレルギー：皮疹，肝障害
エタンブトール(EMB)	細胞壁ミコール酸合成阻害？	視力障害，視神経炎
ピラジナミド(PZA)	pyrazinoic acid 産生	肝障害，高尿酸血症
ストレプトマイシン(SM)	タンパク質合成阻害	第 8 脳神経障害，腎障害

表 IV-59　薬剤耐性結核の出現状況

全体		初回耐性		獲得(再治療)耐性	
いずれの 1 薬剤	多剤耐性	いずれの 1 薬剤	多剤耐性	いずれの 1 薬剤	多剤耐性
12.6%	2.2%	9.9〜10.7%	1.0〜1.4%	23.3〜36.0%	9.3〜13.0%

いずれの 1 薬剤：イソニアジド(INH)，リファンピシン(RIF)，エタンブトール(EMB)，ストレプトマイシン(SM)

5) 治療および予防

治療の原則は多剤併用抗結核化学療法である(表 IV-58)。結核菌の薬剤耐性は，各抗結核薬の標的に関与した遺伝子の変異により獲得され，多剤耐性はこれらの遺伝子の変異が集積することにより，出現する。抗結核薬により，耐性菌出現頻度は異なるが，1 薬剤あたり，$1/10^6$〜10^9 であるため，薬剤を併用することにより，耐性菌の出現頻度を低下させることが可能となる。ただしこの場合，確実に服用することが絶対条件である。そのため，WHO は直接監視下短期化学療法 directly observed treatment, short course(DOTS)を推進している。標準的な治療で，服薬期間は約 6 か月である。組み合わせでは，最初の 2 か月：イソニアジド(INH)＋リファンピシン(RIF)＋エタンブトール(EMB)〔あるいはストレプトマイシン(SM)〕＋ピラジナミド(PZA)，その後 4 か月：INH＋RIF を用いる〔最近の米国疾病管理予防センター Centers for Disease Control and Prevention(CDC)の治療指針では SM 耐性結核菌の増加に伴い，SM は抗結核薬としての選択順位が低下した〕。

薬剤耐性結核 drug-resistant tuberculosis(表 IV-59)の原因は不適切な結核医療，すなわち，抗結核化学療法薬の不適切な選択や使用，治療中断や脱落であり，医療関係者や患者の対応に起因する man-made disease である。全世界で 5,000 万人以上が多剤耐性結核菌(INH と RIF に同時耐性，multidrug-resistant tuberculosis：MDR-TB)に既感染しており，医療費は薬剤感受性結核に比べ，3〜100 倍を要している。MDR-TB の性状に加え，フルオロキノロンとカプレオマイシンの 2 薬剤に耐性，かつ，カナマイシンおよびアミカシンの少なくとも 1 薬剤に耐性である超多剤耐性結核 extensively/extremely drug-resistant tuberculosis(XDR-TB)が最近報告されている。薬剤耐性結核(菌)の出現や蔓延は結核制圧対策における大きな課題である。

予防は，感染源対策として患者の早期発見，治療，接触者(家族，学校，会社など)の調査，さらに，予防接種や化学予防(無症候潜在性結核菌感染の治療)がある。予防接種は弱毒ウシ型結核菌 bacille Calmette-Guérin(BCG)が汎用され，乳幼児結核(全身播種性結核や髄膜結核)の予防に効果(70〜80%)が認められているが，成人型肺結核の予防効果は疑問視されている。化学予防は INH を服用し，発症を防止する(効果：70〜80%)。ただし，感染結核菌が INH 感受性であることが不可欠である。

2007 年 4 月の改正感染症法の施行に伴い，結核予防法は「感染症の予防及び感染症の患者に対する医療に関する法律(感染症法)」に統廃合された。結核は 2 類感染症に位置づけられ，結核を診断した場合，医師は直ちに最寄りの保健所長を経

表 IV-60　非結核性抗酸菌感染症と原因菌

疾患	主要な病原体 (Runyon 分類)	抗菌薬
肺感染症	*M. avium* (III)	クラリスロマイシン，アジスロマイシン，エタンブトール
	M. intracellulare (III)	クラリスロマイシン，アジスロマイシン，エタンブトール
	M. kansasii (I)	リファンピシン，イソニアジド，エタンブトール
	M. abscessus (IV)	アミカシン，シプロフロキサシン，クラリスロマイシン
	M. xenopi (II)	クラリスロマイシン，リファンピシン，エタンブトール
リンパ節炎	*M. avium* (III)	クラリスロマイシン，アジスロマイシン，エタンブトール
	M. intracellulare (III)	クラリスロマイシン，アジスロマイシン，エタンブトール
	M. scrofulaceum (II)	クラリスロマイシン，アジスロマイシン(外科的切除)
皮膚感染症	*M. marinum* (I)	ドキシサイクリン，リファンピシン，エタンブトール
	M. fortuitum (IV)	アミカシン，シプロフロキサシン，クラリスロマイシン
	M. chelonae (IV)	アミカシン，シプロフロキサシン，クラリスロマイシン
	M. abscessus (IV)	アミカシン，シプロフロキサシン，クラリスロマイシン
	M. ulcerans (III)	クラリスロマイシン，リファンピシン，エタンブトール
播種性感染症	*M. avium* (III)	クラリスロマイシン，アジスロマイシン，エタンブトール
	M. intracellulare (III)	クラリスロマイシン，アジスロマイシン，エタンブトール
	M. kansasii (I)	リファンピシン，イソニアジド，エタンブトール
	M. chelonae (IV)	アミカシン，シプロフロキサシン，クラリスロマイシン
	M. abscessus (IV)	アミカシン，シプロフロキサシン，クラリスロマイシン
	M. haemophilum (III)	クラリスロマイシン，リファンピシン，エタンブトール

表 IV-61　主要な非結核性抗酸菌感染症の特徴

菌種	頻度	至適温度(℃)	感染源，経路	抗菌薬感受性
M. avium complex	最頻(70%)	37	水，土壌，鳥類	耐性
M. kansasii	頻(20%)	37	水，土壌	感受性
M. marinum	少ない	30	水，魚類	感受性
M. ulcerans (Buruli 潰瘍)	頻(アフリカ，オセアニア)	30	経皮感染，動物由来？	耐性

由し都道府県知事に届け出なければならない。

b 非結核性抗酸菌感染症
nontuberculous mycobacterial infections

結核菌以外の抗酸菌〔非結核性抗酸菌 nontuberculous mycobacteria (NTM)，非定型抗酸菌 atypical mycobacteria，mycobacteria other than tuberculosis (MOTT)，potentially pathogenic environmental mycobacteria (PPEM) ともいう〕は，環境(土壌や水など)に広く分布し，多くの場合，健常者に対し，病原性を示すことは少ない。したがって，ヒト-ヒト感染はない。わが国では，結核などを含めた全抗酸菌陽性患者の約 20% が非結核性抗酸菌感染症と考えられている(表 IV-60)。

非結核性抗酸菌による肺感染症の原因菌として，*M. avium*，*M. intracellulare*〔*M. avium* と *M. intracellulare* は細菌学的に極めて類似しているため，一括して *M. avium* complex (MAC) と表すことがある〕，*M. kansasii* が多く，MAC が 70〜80%，*M. kansasii* が 20% を占める(表 IV-61)。リンパ節炎は MAC や *M. scrofulaceum*。皮膚感染症は *M. marinum* (魚槽肉芽腫 fish tank granulomas)，*M. fortuitum*，*M. chelonae*，*M. abcessus* や *M. ulcerans* (Buruli 潰瘍)。重度の免疫不全の場合，播種性感染症は MAC，*M. kansasii*，*M. chelonae*，*M. abcessus* や *M. haemophilum* などが多い(表IV-60)。

NTM の易感染性要因として，進行した後天性免疫不全症候群(末梢血 CD4 陽性 T 細胞数≦100/μl)など免疫不全や肺基礎疾患(気管支拡張症，肺嚢胞，塵肺や陳旧性結核など)が知られて

表 IV-62　らい菌の特徴

至適発育温度	30～33°C
遅発育性	分裂倍加時間，11～13 日
らい菌特異的抗原	フェノール抽出性糖脂質(PGL)
感染経路	気道感染 > 経皮感染
好発部位	皮膚および末梢神経(Schwann 細胞親和性)
病変・症状	皮膚：皮疹，結節 神経：知覚・運動障害，神経肥厚

いるが，これらの状況を欠如した症例もしばしば認められる。MAC は多くの抗結核薬に耐性を示すことが多く，比較的有効な新規マクロライド系抗菌薬(クラリスロマイシンやアジスロマイシン)が用いられているが，根治は困難である。なお，*M. kansasii* は通常の抗結核薬(前出)に感受性を示すことが多い。NTM はヒト-ヒト感染しないので，隔離は不要である。

C ハンセン病 leprosy，Hansen's disease

ハンセン病は慢性らい菌感染症である。らい菌の至適発育温度が 30～33°C 前後のため，皮膚，末梢神経，上気道粘膜および眼など体表部に好発する。ハンセン病に特徴的な症状として，① 知覚(触覚，痛覚，温冷覚)障害を随伴した皮疹(斑，丘疹，結節など)，② 末梢神経の肥厚および神経支配領域における知覚または運動障害がある。

1) 発生動向

わが国におけるハンセン病療養所の入所者は約 2,700 人であり，そのほとんどは治癒(らい菌陰性化)しているが，後遺症のため入所している。入所者の高齢化が進み，平均年齢は約 80 歳である。「らい予防法の廃止に関する法律」が 1996(平成 8)年 4 月 1 日より施行されたことにより，患者の届け出が廃止された。したがって，らい予防法廃止後，患者発生動向の詳細は不明であるが，わが国における年間の新規発生患者は 10 人以下(半数以上が在日外国人)である。世界における登録患者は約 22 万人(2006 年)，年間新規発生患者は 26 万人(2006 年)であり，患者の多い国々はインド，ブラジル連邦共和国，マダガスカル共和国，アンゴラ共和国，中央アフリカ共和国，コンゴ民主共和国，モザンビーク共和国，ネパールやタンザニア連合共和国である。ハンセン病流行地域における新規患者は 10～20 歳代と 40～60 歳代にピークがあり，二峰性分布を示すが，わが国を含め低蔓延地域では 60 歳代以降に多い。

表 IV-63　ハンセン病の病型

	類結核型	らい腫型
病変部らい菌数	少菌性	多菌性
免疫応答	細胞性	液性
レプロミン皮内反応(Mitsuda)	陽性	陰性
抗 PGL 抗体	陰性	陽性

2) 病原体

らい菌 *Mycobacterium leprae* は抗酸菌の一種で，細胞内寄生性細菌である(表 IV-62)。しかし，今日までらい菌は試験管内培養に成功していない。らい菌は**グラム陽性，抗酸性**を示し，抗酸菌染色(Ziehl-Neelsen，Kinyoun や Fite 法)により赤染する。らい菌は葉巻タバコ状 bundles of cigars といわれる一定の方向性のもとに散在性，塊状あるいはらい球 globi と呼ばれるらい菌特有の集簇を形成し，マクロファージに貪食され，また，末梢神経の Schwann 細胞に親和性が高く，これらの細胞内で増殖する。世代時間は 11～13 日と考えられ，遅発育菌である結核菌の世代時間(約 12～15 時間)と比較しても著しく発育の遅い菌で，感染した場合，発症までの潜伏期間は数週～数十年(平均 3～5 年)を要する。至適発育温度は 30～33°C 前後，感染のための最少菌数は 3～40 個といわれているが，病原性は極めて弱い。らい菌に対する宿主防御機構は T 細胞が中心的役割を果たす細胞性免疫である。らい菌は経気道および経皮的に感染するが，らい菌の病原性は極めて弱く，感染しても発病することはまれである。

3) 臨床症状

ハンセン病の病型分類は，基本的にらい腫型 lepromatous と類結核型 tuberculoid から構成される(表 IV-63)。また，経過中に急性症状を呈することがあり，**らい反応**と総称する。

① らい腫型 lepromatous(図 IV-60)

らい菌に対する細胞性免疫応答を欠如し，そのため，多数のらい菌を病変部に認める(多菌型 multibacillary)。症状として，斑，丘疹，結節(らい腫)などの皮疹が混在して対称性に多数生じ，進行性である。また，末梢神経症状として，知覚

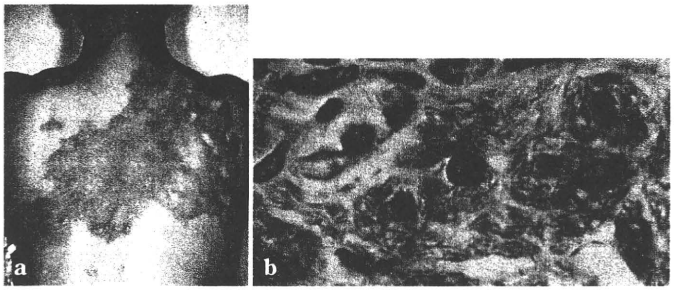

図Ⅳ-60　ハンセン病(らい腫型)の皮膚病変(a)と組織学的所見(b)
b：Ziehl-Neelsen 染色，らい菌特有の集簇：らい球 globi を多数認めた。

障害や発汗障害をしばしば認めるが，神経肥厚は顕著でないことが多い。

② 類結核型 tuberculoid

らい菌に対する細胞性免疫応答が強く，病変部にらい菌はほとんど存在しない(少菌型 paucibacillary)。通常，経過は良好で，安定している。境界明瞭な斑(紅斑，色素脱失斑など)が主であり，限局した1〜数個の皮疹が非対称性に出現する。神経肥厚はしばしばみられ，部位では尺骨，大耳介や腓腹神経に好発する。そのため，支配領域の知覚・運動障害を生じることが多い。

③ らい反応

ハンセン病は，通常，慢性に経過するが，時に急性症状を呈することがあり，らい反応と総称する。境界群に発生する境界反応とらい腫型に発生するらい性結節性紅斑反応がある。末梢神経障害，眼(虹彩毛様体炎，ぶどう膜炎)，免疫複合体性糸球体腎炎など重大な合併症をきたすことがあるので迅速な処置が必要であり，さらに入院加療を要することもある。

4) 診断

病原体診断が確定診断となるが，臨床所見(皮膚および末梢神経病変)に加えて，らい菌が培養不能であることや少菌型(類結核型)を考慮して総合的に進める。

① 細菌学的検査

皮膚や鼻粘膜擦過面からの組織液，病変部組織やホモジネートを抗酸菌染色し，光学顕微鏡的観察により，らい菌を検出する。

② 病理組織学的検査

病変部と健常部を含めて生検し，各種組織染色および抗酸菌染色標本を光学的顕微鏡観察する(図Ⅳ-60)。

③ 特異的抗体検査

らい菌に特有なフェノール抽出性糖脂質(PGL)に対する血清抗体を検出する。この抗体はらい腫型に陽性であるが，類結核型では陰性であることが多い。

④ らい菌特異的遺伝子増幅検査

ポリメラーゼ連鎖反応(PCR)を利用し，らい菌特異的遺伝子を検出する。

⑤ レプロミン皮内反応

らい菌に対する細胞性免疫応答を調べるものであり，ハンセン病の病型分類には有用であるが，診断には通常用いない。らい腫型ハンセン病に陰性であるが，類結核型では陽性であることが多い。

5) 治療および予防

確実な治癒と耐性菌出現を防止するため原則として，多剤併用化学療法を行う。標準的な多剤併用化学療法として，リファンピシン，ジアフェニルスルホン，クロファジミンを投与する。

なお，らい反応のために化学療法薬を中止したり，変更する必要は通常ない。らい反応が出現した場合，炎症反応を抑制するために，非ステロイド性抗炎症薬，副腎皮質ステロイド薬や TNF-α の拮抗薬であるサリドマイドなどが用いられる。なお，サリドマイドは催奇形性を有しているため，妊婦には禁忌である。

1996(平成8)年4月より「らい予防法」が廃止され，患者の届け出，隔離，消毒や行動制限などは撤廃された。　(小林和夫)

C 抗酸菌（マイコバクテリア）感染症

190 結核（非結核性〈非定型〉抗酸菌症）

1. 概念

結核は結核菌群 *Mycobacterium tuberculosis complex*（*M. tuberculosis*, *M. bovis* や *M. africanum*）を起炎菌とする慢性感染症であり，ほとんどは結核菌 *M. tuberculosis* による．日本の新規発生結核患者数（2007年）は約2.5万人，罹患率19.8（対人口10万人）であり，現在においても甚大な健康被害を及ぼしている．病変部位により，肺結核，肺外結核，粟粒（全身播種性）結核に分類される．結核菌群および培養不能のらい菌 *M. leprae*（ハンセン病の原因菌）を除く他の *Mycobacterium*（抗酸菌）属が非結核性〈非定型〉抗酸菌であり，結核を含む全抗酸菌感染症の15～20％を占める．*M. avium - intracellulare*（MAI/MAC）が最頻（70％），次いで *M. kansasii*（20％），散発的に *M. chelonae, M. fortuitum, M. gordonae, M. scrofulaceum, M. szulgai* などが原因菌となる．抗酸菌細胞壁は脂質に富むため Ziehl-Neelsen 法や蛍光などの特殊染色（抗酸性染色）を行う．しかし，一旦染色されると塩酸などでも脱色され難いことから抗酸菌（acid-fast bacilli）と呼ぶ．抗酸菌はグラム陽性好気性桿菌で一般的に遅発育性である（固形培地で集落形成は1週間以上）．結核菌群は生化学的にナイアシンを産生し，他の抗酸菌と区別される．結核，非結核性抗酸菌症ともにHIV感染症／AIDSにおける日和見感染症としても重要である．また，抗微生物薬耐性結核菌や非結核性抗酸菌の出現頻度が増加し，化学療法に抵抗性を示すこともある．結核の予防ワクチンとして弱毒ウシ型結核菌由来生ワクチンの BCG が汎用されている．乳幼児における BCG 接種は有効であり，生後6カ月までに直接接種する（予防接種法）．しかし，成人への効果は疑問視されているため，通常，再接種は不要である．

2. 病態生理

喀痰に含まれる結核菌の飛沫核（空気）感染により，結核はヒト－ヒト感染伝播する．感染しても発病は生涯を通じて約10％で，90％は感染した結核菌が休眠状態 dormancy で宿主体内に残存する（persister）．結核菌は細胞内寄生菌であるため，宿主マクロファージに貪食された後，殺菌されずに増殖する．一部は肺門など，所属リンパ節に運ばれる．感染部位にはマクロファージ・リンパ球が集積し，肉芽腫を形成するが，マクロファージは形態学的に類上皮細胞や Langhans 多核巨細胞を呈する．さらに，病巣中心部は乾酪壊死を起こす．これを初期変化群と呼ぶ．細胞性免疫が十分で病巣が小さい場合，石灰沈着を伴い治癒する．そのまま進展すれば初感染結核が起こる．一部は乾酪性肺炎になり，乾酪用物質が排出され空洞が形成されることがある．胸膜に波及し，胸水を伴う浸出性炎症を起こす．肺門リンパ節内の菌はリンパ行性に静脈角リンパ節を経由し，血行に入り菌血症を起こす．すなわち，全身播種性（粟粒性）結核である．微量の菌の場合，菌が運ばれた先の臓器に結核病変を形成する．二次結核症は初期病変の内因性再燃により生じるが，既に成立している免疫の存在下で起こる．リンパ節の関与は少なく，増殖性の関与が強く，空洞形成が起こる．空洞内は酸素が豊富で大量の菌が増殖し，感染源および肺内散布の原因となる．

非結核性抗酸菌は環境（土壌，水など）からヒトへ感染すると考えられるが，通常，ヒト-ヒト感染はない．発病は稀で，日和見的に発症する．AIDSなど免疫不全の場合，全身播種性病変，顕著な免疫不全がない場合，中年以降の女性に好発する．

3. 臨床症状

2週間以上持続する咳嗽，喀痰や発熱が最も多い．全身倦怠，血痰，胸痛，体重減少，寝汗や食欲低下などを伴うこともある．なお，約20％は自覚症状の有無にかかわらず，健康診断で発見される．

4. 検査・診断（表1）

a. 感染病原体の検出や同定が最も重要であり，結核の場合，確定診断となる．

1）集菌法による喀痰塗抹検査

Ziehl-Neelsen 法や蛍光染色，3回連続検痰を行う．

2）培養法

固形培地：小川培地，Lowenstein－Jensen 培地，Middlebrook 7 H 10 や 7 H 11

液体培地：MGIT や MB check

表1　結核の診断

病原体診断	塗抹検査	抗酸菌染色（Ziehl-Neelsen，Kinyoun 染色），蛍光染色
	培養検査	固形培地（卵培地：小川，Lowenstein-Jensen，寒天培地：Middlebrook 7 H 10，7 H 11）：4～8週間 液体培地（MGIT，MB check）：7～14日 薬剤感受性試験
	遺伝子検出	核酸増幅法：polymerase chain reaction（PCR） DNA-DNA ハイブリゼーション 薬剤耐性遺伝子
補助診断	胸部X線	中および上肺野病変（浸潤，結節や空洞） リンパ節腫大や石灰化 胸膜炎／胸水貯留
	病理学的検査	乾酪壊死を伴う肉芽腫
	TST	ツベルクリン皮内反応（Mantoux） 48時間後判定：遅延型皮内反応 陽性：結核菌感染，BCG陽転，非結核性抗酸菌感染 陰性：未感染，BCG未接種，免疫不全（HIV/AIDS，重症結核，薬物性）
	IGRA：QFT	末梢血細胞 IFN-γ 産生・遊離試験（IGRA，Quantiferon）：In vitro 抗原；ESAT-6，CFP-10

培養期間：固形培地4週間以上，液体培地1週間以上

3）生化学試験法

極東抗酸菌鑑別キットやキャピリア TB

4）遺伝子検査法

PCR など核酸増幅法，DNA プローブ法や DNA-DNA ハイブリゼーション法

b. 補助的：陽性，あるいは，陰性所見を問わず，確定診断でないことに留意

1）画像診断

胸部X線や CT 検査：上中肺野を中心として散布を伴う不規則，大小不同の陰影，空洞，石灰化・癒着像，胸水貯留，粟粒陰影，肺門リンパ腫腫大

2）病理組織学的検査

乾酪壊死を伴う肉芽腫病変

3）免疫学的診断法

ツベルクリン皮内反応：精製ツベルクリン皮内注射，紅斑径 10 mm 以上が陽性

結核菌特異抗原による末梢血単核細胞interferon-γ遊離試験（IGRA，QuantiFERON）：0.35 IU/mL 以上が陽性

c. 薬剤感受性試験

小川培地や液体培地を用いた薬剤感受性試験

d. 非結核性抗酸菌症の検査・診断（米国胸部疾患および感染症学会の診断基準 2007 年）

環境菌のため，診断には画像診断（胸部X線や CT 検査），非結核性抗酸菌の検出および他疾患の除外を要する．

e. 届出など行政対応

「感染症の予防及び感染症患者に対する医療に関する法律」の規程により，結核を診断した医師は最寄りの保健所長に直ちに届け出る．なお，非結核性抗酸菌症は法律の対象外であり，届出は不要である．

5. 治療

確実な治療や薬剤耐性菌の出現防止のため，多剤を併用した直接監視下短期抗結核化学療法（DOTS：イソニアジド，リファンピシン，エタンブトール＋ピラジナマイドの4薬剤を最初の2カ月間投与，イソニアジド＋リファンピシンの2薬剤を残りの4カ月間，合計6カ月間）が推奨されている．近年，多剤耐性（MDR）結核（イソニアジドとリファンピシンに同時耐性），超多剤耐性（XDR）結核（MDR でフルオロキノロン耐性，かつ，カナマ

イシン，アミカシン，カプレオマイシンなど注射可能薬の少なくとも１剤以上に耐性）が問題となっている．

非結核性抗酸菌症，特にMAC感染症では抗微生物薬耐性もしばしばであり，マクロライド系薬が推奨される．なお，*M. kansasii* 感染症は通常，抗結核薬に感受性である．

薬剤耐性の場合，感受性試験結果や臨床的反応性を総合し，化学療法を実施する．

病変（肺葉や肺）切除など，外科的適応はMDR-，XDR-結核やMAC感染症で心肺機能の良好な限局性肺病変や孤発性単一結節性病変に考慮する．

6．予後

薬剤感受性結核，かつ適切な化学療法を実施した場合，再発率は５％以下である．再発は治療完了後１年以内に出現することが多い．再発の危険性が大きいと考えられる場合，少なくとも２年間，胸部X線検査，喀痰検査などの観察を行う．薬剤耐性，特に，XDR-結核は予後不良である．

Lipocalin 2-Dependent Inhibition of Mycobacterial Growth in Alveolar Epithelium[1]

Hiroyuki Saiga,*† Junichi Nishimura,* Hirotaka Kuwata,† Megumi Okuyama,* Sohkichi Matsumoto,‖ Shintaro Sato,§ Makoto Matsumoto,† Shizuo Akira,§¶ Yasunobu Yoshikai,‡ Kenya Honda,* Masahiro Yamamoto,* and Kiyoshi Takeda[2]*†¶

Mycobacterium tuberculosis **invades alveolar epithelial cells as well as macrophages. However, the role of alveolar epithelial cells in the host defense against *M. tuberculosis* remains unknown. In this study, we report that lipocalin 2 (Lcn2)-dependent inhibition of mycobacterial growth within epithelial cells is required for anti-mycobacterial innate immune responses. Lcn2 is secreted into the alveolar space by alveolar macrophages and epithelial cells during the early phase of respiratory mycobacterial infection. Lcn2 inhibits the in vitro growth of mycobacteria through sequestration of iron uptake. Lcn2-deficient mice are highly susceptible to intratracheal infection with *M. tuberculosis*. Histological analyses at the early phase of mycobacterial infection in Lcn2-deficient mice reveal increased numbers of mycobacteria in epithelial cell layers, but not in macrophages, in the lungs. Increased intracellular mycobacterial growth is observed in alveolar epithelial cells, but not in alveolar macrophages, from Lcn2-deficient mice. The inhibitory action of Lcn2 is blocked by the addition of endocytosis inhibitors, suggesting that internalization of Lcn2 into the epithelial cells is a prerequisite for the inhibition of intracellular mycobacterial growth. Taken together, these findings highlight a pivotal role for alveolar epithelial cells during mycobacterial infection, in which Lcn2 mediates anti-mycobacterial innate immune responses within the epithelial cells.** ***The Journal of Immunology,*** **2008, 181: 8521–8527.**

Tuberculosis is a worldwide disease caused by infection with *Mycobacterium tuberculosis*. Therefore, the host defense mechanisms against *M. tuberculosis* have been intensively investigated, and important roles of T cell-mediated adaptive immunity have been well established (1, 2). In addition, functional characterization of TLRs has recently indicated the importance of innate immunity in the host responses to infection with *M. tuberculosis* (3, 4). In the TLR-mediated anti-mycobacterial immune responses, macrophages and dendritic cells are major effectors that engulf pathogens and produce a variety of proinflammatory mediators. In respiratory mycobacterial infection, alveolar macrophages are the major targets of invasion. However, several evidences indicate that mycobacteria also interact with epithelial cells in the respiratory tract and invade these cells (5–9). Accordingly, epithelial cells in the lungs are expected to play a role during mycobacterial infection by producing antimicrobial mediators (10).

Lipocalin 2 (Lcn2),[3] also known as neutrophil gelatinase-associated lipocalin, siderocalin, 24p3, or uterocalin, a member of the lipocalin family of proteins that bind to small hydrophobic molecules, is produced by epithelial cells and macrophages (11–16). Lcn2 has been shown to mediate several biological processes, including mammary gland involution, induction of apoptosis, and delivery of iron (12, 17–19). In addition, structural studies have demonstrated that Lcn2 binds to enterobactin-type bacterial siderophores, which facilitate iron uptake by bacteria (16). Subsequent studies revealed that Lcn2 also binds to other types of siderophores, such as carboxy-mycobactin (produced by mycobacteria) and bacillibactin (produced by *Bacillus anthracis*) (20, 21). Lcn2 has been shown to interfere with siderophore-mediated iron uptake in *Escherichia coli* (16). Accordingly, mice deficient in Lcn2 are highly susceptible to infection with *E. coli* (22, 23). Thus, Lcn2 mediates the host defense against *E. coli* infection through sequestration of iron, which is essential for the growth and activity of nearly all bacteria (24).

Mycobacteria replicate within cells, especially in the phagosome of macrophages (25), where iron is limited. Outside host cells, free iron is also limited, because almost all iron ions exist as complexes with host proteins with high affinity for iron, such as transferrin and lactoferrin. To overcome the iron deficiency within the host, some species of mycobacteria, such as *M. tuberculosis* and *Mycobacterium bovis* bacillus Calmette-Guérin (BCG), synthesize two type of siderophores, called mycobactin and carboxy-mycobactin (also called exochelin) (26, 27). Mycobactin is hydrophobic, whereas carboxy-mycobactin is hydrophilic. These mycobactins have been shown to remove iron from host iron-binding proteins, such as transferrin and lactoferrin (28). In addition, *M. tuberculosis*

*Laboratory of Immune Regulation, Department of Microbiology and Immunology, Graduate School of Medicine, Osaka University, Suita, Osaka, Japan; †Department of Molecular Genetics and ‡Division of Host Defense, Research Center for Prevention of Infectious Diseases, Medical Institute of Bioregulation, Kyushu University, Fukuoka, Japan; §Department of Host Defense, Research Institute for Microbial Diseases and ¶WPI Immunology Frontier Research Center, Osaka University, Suita, Osaka, Japan; and ‖Department of Bacteriology, Osaka City University Graduate School of Medicine, Osaka, Japan

Received for publication August 5, 2008. Accepted for publication October 11, 2008.

The costs of publication of this article were defrayed in part by the payment of page charges. This article must therefore be hereby marked *advertisement* in accordance with 18 U.S.C. Section 1734 solely to indicate this fact.

[1] This work was supported by a Grant-in-Aid from the Ministry of Education, Culture, Sports, Science and Technology and the Ministry of Health, Labor and Welfare, as well as the Osaka Foundation for the Promotion of Clinical Immunology.

[2] Address correspondence and reprint requests to Dr. Kiyoshi Takeda, Laboratory of Immune Regulation, Department of Microbiology and Immunology, Graduate School of Medicine, Osaka University, Suita, Osaka, Japan. E-mail address: ktakeda@ongene.med.osaka-u.ac.jp

[3] Abbreviations used in this paper: Lcn2, lipocalin 2; BCG, *Mycobacterium bovis* bacillus Calmette-Guérin; BALF, bronchoalveolar lavage fluid; rLcn2, recombinant Lcn2; SP-C, pro-surfactant protein C; DFO, deferoxamine; AEC, alveolar epithelial cell; CPZ, chlorpromazine.

Copyright © 2008 by The American Association of Immunologists, Inc. 0022-1767/08/$2.00

with mutations in the *mbtB* gene, which lack carboxy-mycobactin and mycobactin, exhibit impaired replication in low-iron medium and within macrophages (27). The mechanisms for the mycobactin-mediated iron acquisition within the phagosome of macrophages have recently been elucidated (29). Because pulmonary epithelial cells are also invaded by mycobacteria, host defense mechanisms that inhibit mycobacterial replication within these cells are expected to exist, however they currently remain unclear.

In the present study, we analyzed the role of Lcn2 in mycobacterial infection. Lcn2, which inhibits mycobacterial growth, was rapidly produced from alveolar macrophages and epithelial cells after mycobacterial infection. Furthermore, analyses using Lcn2-deficient mice revealed a pivotal role of alveolar epithelial cells in mycobacterial infection.

Materials and Methods

Mice

Lcn2$^{-/-}$ and *H-2K*^{b}*-tsA58* transgenic mice have been generated (22, 30) and backcrossed to C57BL/6 for six generations. *Lcn2*$^{-/-}$ and wild-type littermates from intercrosses of *Lcn2*$^{+/-}$ mice were used for experiments at 6–8 wk of age. All animal experiments were conducted in accordance with the guidelines of the Animal Care and Use Committee of Kyushu University and Osaka University.

Mycobacteria

M. bovis BCG (Tokyo strain) was purchased from Kyowa Pharmaceuticals. *M. tuberculosis* strains H37Ra (ATCC25177) and H37Rv (ATCC358121) were grown in Middlebrook 7H9-ADC medium for 2 wk and stored at −80°C until use. GFP-expressing BCG, which was generated previously (5), was used for the experiment.

Quantitative real-time RT-PCR

Total RNA was isolated with the TRIzol reagent (Invitrogen), and reverse transcribed using M-MLV reverse transcriptase (Promega) and random primers (Toyobo) after treatment with RQ1 DNaseI (Promega). Quantitative real-time PCR was performed in ABI7300 (Applied Biosystems) using TaqMan Universal PCR Master Mix (Applied Biosystems). All data are shown as the relative mRNA levels normalized by the corresponding 18S rRNA level. The primers for 18S rRNA and Lcn2 were purchased from Assays on Demand (Applied Biosystems).

Preparation of alveolar macrophages

Bronchoalveolar lavage fluid (BALF) was collected from uninfected mice. To eliminate contamination by bacteria, the cells were cultured with 50 U/ml penicillin and 50 μg/ml streptomycin for 16 h, and then washed five times to remove nonadherent cells. The resultant adherent cells were used for experiments as alveolar macrophages, because >95% of the adherent cells were CD11b-positive.

Preparation of recombinant Lcn2 (rLcn2) protein

A mouse Lcn2 cDNA fragment was inserted into pGEX6P-2 (GE Healthcare) and transformed into *E. coli* BL21. The expressed GST-Lcn2 fusion proteins were purified using glutathione-Sepharose 4B (GE Healthcare) according to the manufacturer's instructions. The purified proteins were incubated with PreScission Protease (GE Healthcare) to cleave the GST tag, and then purified with Glutathione-Sepharose 4B.

Immunohistochemistry

Lungs were fixed with 4% PFA and frozen in Tissue-Tec OCT compound (Sakura). The sections were incubated with anti-mouse Lcn2 Ab (R&D Systems), anti-pro-surfactant protein C (SP-C) Ab (Chemicon), anti-CD11b Ab (BD Biosciences), or anti-pan cytokeratin Ab (Sigma-Aldrich). The nuclei were stained with 4′,6-diamidino-2-phenylindole (DAPI; Molecular Probes). Alveolar epithelial cells were infected with GFP-expressing BCG for 16 h, washed, and incubated with Dextran Conjugates (Cascade Blue; Molecular Probes) and Alexa Fluor 594-labeled rLcn2 for 6 h. rLcn2 was labeled using an Alexa Fluor 594 Protein Labeling Kit (Molecular Probes). The cells were fixed with 4% PFA and analyzed using a confocal microscopy (LSM 510; Carl Zeiss).

Western blot assay

BALF was collected from BCG-infected mice by catheterization techniques into 500 μl of PBS. To normalize BALF samples, we injected the same volume of PBS (500 μl), recovered equal volume, and used them for Western blot analysis. After removal of precipitates, the samples were separated on SDS-PAGE and transferred to PVDF membranes (Millipore). The membranes were incubated with anti-mouse Lcn2 Ab. Bound Ab was detected with SuperSignal West Pico Chemiluminescent Substrate (Pierce).

In vitro mycobacterial growth assay

Mycobacteria were incubated in Middlebrook 7H9-ADC medium with the indicated concentrations of rLcn2 protein for 20 days at 37°C, and were plated on Middlebrook 7H10-OADC agar plates and incubated at 37°C for 30 days. In some experiments, BCG was incubated with the indicated concentrations of deferoxamine mesylate (DFO; Calbiochem), $FeCl_3$ or mycobactin (Kyoritsu Seiyaku) on 7H10-OADC agar plates.

In vivo infection of mycobacteria

Mice were intratracheally infected with *M. tuberculosis* H37Rv (1×10^6 CFU). At 6 wk after infection, homogenates of the lungs and livers were plated on 7H10-OADC agar plates. For histological analyses, the lungs were fixed with 4% PFA at 20 or 5 days after infection, embedded in paraffin, cut into sections, and stained with H&E or by the Ziehl-Neelsen method, respectively.

Establishment of alveolar epithelial cell lines

To establish alveolar epithelial cell lines (AECs) from wild-type and *Lcn2*$^{-/-}$ mice, the mice were crossed with *H-2K*^{b}*-tsA58* transgenic mice, and used for experiments at 4 wk of age. Mouse pulmonary type II AECs were established as previously described (32). The cells were incubated at 33°C and passaged over ten times. The cells were then stained with anti-SP-C Ab to confirm that they were type II alveolar epithelial cells.

In vitro infection of mycobacteria

Wild-type or *Lcn2*$^{-/-}$ derived AECs or alveolar macrophages were incubated with BCG for the indicated periods. To eliminate extracellular BCG, the cells were cultured with 50 μg/ml streptomycin for 1 h, washed three times, and harvested. Lysates of the cells were plated on 7H10-OADC agar plates.

Detection of intracellular growth of mycobacteria

Wild-type and *Lcn2*$^{-/-}$-derived AECs were seeded onto 96-well plates, and infected with BCG for 6 h. To eliminate extracellular BCG, the AECs were cultured with 50 μg/ml streptomycin for 1 h, vigorously washed three times. The cells were pulsed with 37 kBq of [^{3}H]uracil and cultured for 48 h. The cells were harvested on glass fiber filters and the incorporated [^{3}H]uracil was measured using a liquid scintillation counter (Wallac). In some experiments, cytochalasin B (Sigma-Aldrich) or chlorpromazine (CPZ; Calbiochem) was added to the wells at 30 min before the [^{3}H]uracil pulse or rLcn2 addition.

Statistical analysis

Differences between control and experimental groups were evaluated using Student's *t* test or ANOVA plus posthoc testing. Values of $p < 0.05$ were considered to indicate statistical significance.

Results

Expression of lipocalin 2 in BCG-infected lungs

To assess the role of Lcn2 in mycobacterial infection, we first analyzed the expression of Lcn2 in the lungs of C57BL/6 mice intratracheally infected with BCG. Total RNA was extracted from the lungs at 2, 7, and 14 days after infection, and analyzed for Lcn2 mRNA expression by real-time quantitative PCR (Fig. 1*A*). Expression of Lcn2 mRNA was markedly increased at 2 days after infection and decreased thereafter. Because Lcn2 mRNA expression was shown to be induced in macrophages stimulated with TLR ligands (22), we analyzed whether alveolar macrophages expressed Lcn2 mRNA (Fig. 1*B*). Alveolar macrophages were isolated, infected with BCG, and analyzed for Lcn2 mRNA expression at 2 days

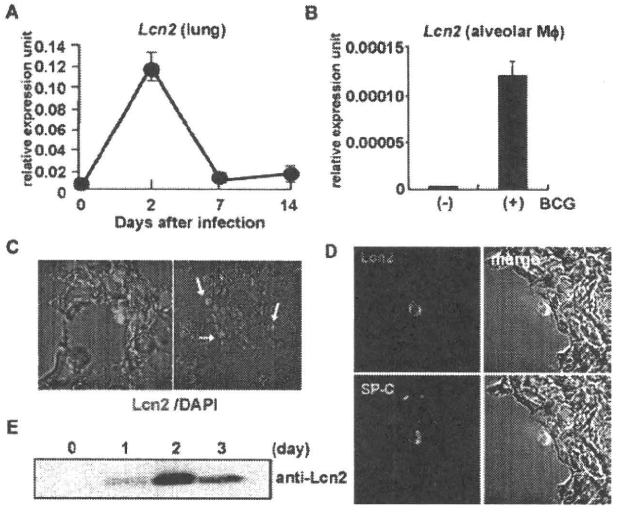

FIGURE 1. Lcn2 expression in the lungs of BCG-infected mice. *A*, Wild-type C57BL/6 mice were intratracheally infected with 2.5×10^6 CFU of BCG. Total RNA was extracted from the lungs after the indicated periods. Lcn2 mRNA expression was analyzed by real-time quantitative PCR. Data are shown as the relative mRNA levels normalized by the corresponding 18S rRNA level. Data are presented as means ± SD, and are representative of two independent experiments. *B*, Alveolar macrophages were isolated from uninfected wild-type mice, cultured with or without BCG for 48 h, and then analyzed for their Lcn2 mRNA expression by real-time quantitative PCR. *C* and *D*, At 2 days after intratracheal infection with BCG, lung tissue sections were stained with anti-Lcn2 Ab (red), DAPI (blue), and anti-SP-C Ab (green), and visualized by fluorescence microscopy. *E*, Wild-type mice were intratracheally infected with 2.5×10^6 CFU of BCG. At the indicated time points after the infection, 500 μl of PBS was intratracheally injected and then recovered. The recovered BALF samples were subjected to Western blot analysis with anti-Lcn2 Ab.

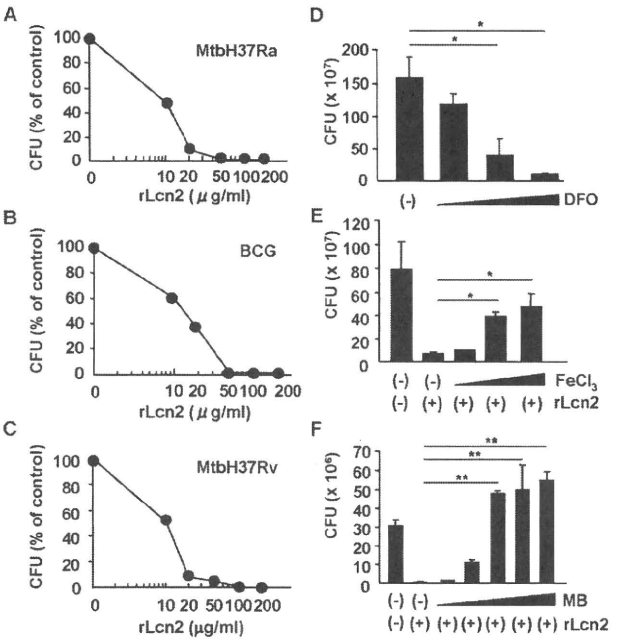

FIGURE 2. Inhibition of in vitro mycobacterial growth by Lcn2. *A–C*, *M. tuberculosis* H37Ra (*A*), BCG (*B*), or *M. tuberculosis* H37Rv (*C*) (1×10^6 CFU each) was incubated with the indicated concentrations of rLcn2 in 7H9 ADC medium for 20 days and then plated on 7H10-OADC agar. The CFU numbers were counted. *D*, BCG was incubated with increasing concentrations of DFO (1 μM, 100 μM and 1 mM) for 20 days and then plated on 7H10-OADC agar. The CFU numbers were counted. *E* and *F*, BCG was incubated in the presence of rLcn2 (50 μg/ml) as well as increasing concentrations of $FeCl_3$ (*E*: 5 nM, 500 nM, 50 μM, and 5 mM) or MB (*F*: 1 pg/ml, 10 pg/ml, 1 ng/ml, 100 ng/ml, and 10 μg/ml) (*F*) for 20 days, and then plated on 7H10-OADC agar. All data are presented as means ± SD. * and ** indicate a significant difference among groups, ANOVA, posthoc Scheffe; *, $p < 0.05$; **, $p < 0.005$.

after infection; BCG infection led to a marked increase in the expression of Lcn2 mRNA. We also analyzed the lungs by immunohistochemistry using an anti BCG-infected mice, several Lcn2-positive cells were observed. These cells mainly faced the alveolar surface and projected into the alveolar space, representing the typical morphology of type II alveolar epithelial cells. Costaining with an Ab to pro-SP-C, which is produced by type II alveolar epithelial cells, revealed that both Lcn2 and SP-C were produced by the same cells (Fig. 1*D*). These findings indicate that not only alveolar macrophages but also type II alveolar epithelial cells produce Lcn2 during respiratory mycobacterial infection. Type II alveolar epithelial cells are known to secrete several mediators into the alveolar space. Therefore, we analyzed whether Lcn2 is secreted into the alveolar space during intratracheal BCG infection. BALF was collected from uninfected and BCG-infected mice and analyzed for Lcn2 protein expression by Western blotting (Fig. 1*E*). Lcn2 was not detected in BALF from uninfected mice. At 2 days after BCG infection, Lcn2 expression was abundantly detected in BALF from the infected mice, indicating that Lcn2 was secreted into the alveolar space during the early phase of mycobacterial infection.

Lcn2-mediated inhibition of mycobacterial growth

We produced rLcn2 and analyzed its effect on in vitro mycobacterial growth. Addition of rLcn2 dose-dependently inhibited the growth of avirulent strains of mycobacteria such as BCG and *M. tuberculosis* H37Ra (Fig. 2, *A* and *B*). rLcn2 also inhibited the growth of virulent *M. tuberculosis* H37Rv in a dose-dependent manner (Fig. 2*C*). Thus, Lcn2 has the ability to inhibit the growth of several mycobacterial strains.

We investigated whether Lcn2 inhibits mycobacterial growth by interfering with iron acquisition, similar to the case for inhibition of *E. coli* growth (16). First, we added DFO, an iron chelator, into in vitro BCG cultures (Fig. 2*D*). DFO reduced BCG growth in a dose-dependent manner, indicating that BCG requires iron for growth. Next, we added ferric iron into BCG cultures (Fig. 2*E*). Addition of ferric iron rescued Lcn2-mediated inhibition of BCG growth in a dose-dependent manner, indicating that Lcn2 inhibits use of iron from the culture medium. Addition of exogenous mycobactin (MB) also abolished Lcn2-mediated inhibition of BCG growth (Fig. 2*F*). These findings indicate that Lcn2 inhibits mycobacterial growth by sequestering iron.

In vivo anti-mycobacterial activity of lipocalin 2

We next addressed the in vivo role of Lcn2 in *M. tuberculosis* infection using $Lcn2^{-/-}$ mice. Wild-type and $Lcn2^{-/-}$ mice were intratracheally infected with *M. tuberculosis* H37Rv and monitored for their survival (Fig. 3*A*). $Lcn2^{-/-}$ mice were highly sensitive to intratracheal infection with *M. tuberculosis* and many of the infected mice died. We also counted the CFU numbers in the lungs and livers after 6 wk of infection (Fig. 3*B*). The CFU titer of *M. tuberculosis* was higher in $Lcn2^{-/-}$ mice than that in wild-type mice. Histopathological analysis of the lungs of the infected mice at 20 days after infection revealed that the number and size of the granulomatous lesions were increased in $Lcn2^{-/-}$ mice (Fig. 3*C*), indicating that the inflammatory response in $Lcn2^{-/-}$ mice was enhanced, possibly due to progression of the *M. tuberculosis* infection. These findings demonstrate that Lcn2 plays an important role in host resistance to *M. tuberculosis* infection in vivo.

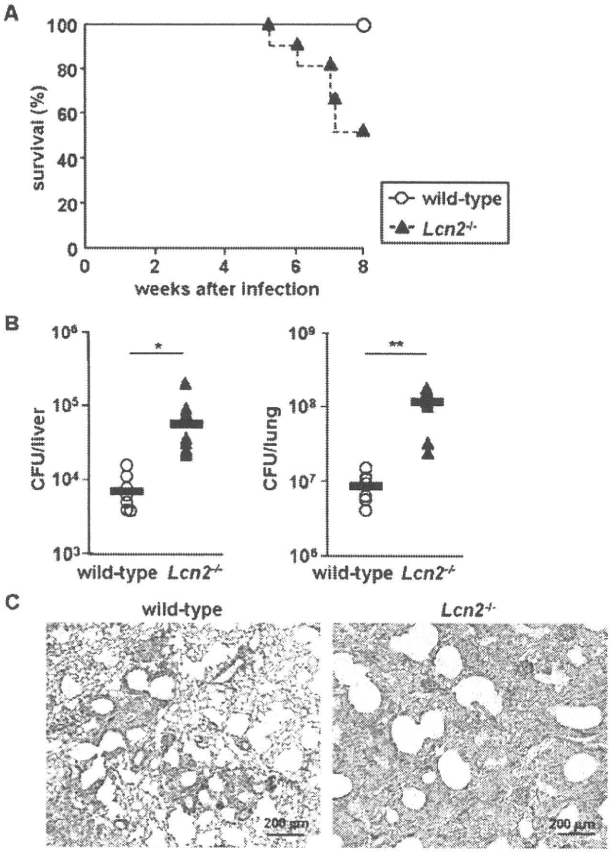

FIGURE 3. High susceptibility of $Lcn2^{-/-}$ mice to *M. tuberculosis* infection. *A*, Wild-type ($n = 11$) and $Lcn2^{-/-}$ ($n = 12$) mice were intratracheally infected with *M. tuberculosis* H37Rv (1×10^6 CFU) and their survival was monitored for 8 wk. *B*, Wild-type ($n = 7$) and $Lcn2^{-/-}$ ($n = 7$) mice were intratracheally infected with *M. tuberculosis* H37Rv (1×10^6 CFU). At 6 wk after infection, homogenates of the lungs and livers were plated on 7H10-OADC agar and the CFU titers were counted. Symbols represent individual mice, and bars represent the mean CFU numbers. *, $p < 0.05$; **, $p < 0.005$. Data are representative of two independent experiments. *C*, H&E staining of representative lung tissues from wild-type and $Lcn2^{-/-}$ mice at 20 days after intratracheal infection with *M. tuberculosis*.

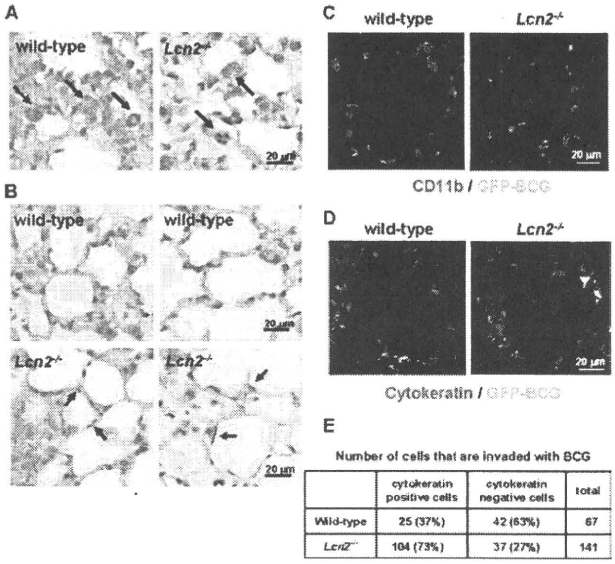

FIGURE 4. Increased numbers of *M. tuberculosis* in $Lcn2^{-/-}$ alveolar epithelial cells. *A* and *B*, Wild-type and $Lcn2^{-/-}$ mice were intratracheally infected with *M. tuberculosis* H37Ra. At 5 days after infection, the lungs were fixed in paraffin, sectioned, and stained with the Ziehl-Neelsen method. Arrows indicate red-stained *M. tuberculosis*. *C–E*, At 5 days after intratracheal infection with GFP-expressing BCG (green), lung tissue sections were stained with anti-CD11b Ab (*C*, red) or anti-pan-cytokeratin Ab (*D*, red), and visualized by fluorescence microscopy. The number of cells containing BCG was counted in a total of ten areas of pictures that visualized different fields (*E*).

Increased numbers of mycobacteria in Lcn2-deficient alveolar epithelial cells

We next analyzed the localization of *M. tuberculosis* in the lungs at 5 days after intratracheal infection by staining acid-fast bacilli using the Ziehl-Neelsen method. In wild-type and $Lcn2^{-/-}$ mice, similar densities of *M. tuberculosis* were observed in granulomatous lesions, although the number and size of the granulomatous lesions were increased in $Lcn2^{-/-}$ mice (data not shown). In addition, *M. tuberculosis* exhibited similar staining of cells with a macrophage-like morphology in wild-type and $Lcn2^{-/-}$ mice (Fig. 4*A*). Strikingly, some of the alveolar epithelial cell layers in $Lcn2^{-/-}$ mice contained *M. tuberculosis* (Fig. 4*B*). In sharp contrast, *M. tuberculosis* was scarcely detected within the epithelial cell layers of wild-type mice. To corroborate these findings, we subjected the lungs of mice intratracheally infected with GFP-expressing BCG to immunohistochemical analyses. In both wild-type and $Lcn2^{-/-}$ mice, CD11b-positive cells contained GFP-expressing BCG. However, in the lungs of $Lcn2^{-/-}$ mice, GFP-expressing BCG was frequently observed in cells that did not express CD11b, in contrast to the low frequency observed in the lungs of wild-type mice (Fig. 4*C*). Visualization of epithelial cells using an anti-cytokeratin Ab indicated that increased numbers of alveolar epithelial cells in $Lcn2^{-/-}$ mice contained GFP-expressing BCG compared with those in wild-type mice (Fig. 4, *D* and *E*). Thus, in the absence of Lcn2, invasion and replication of mycobacteria in alveolar epithelial cells were increased.

Therefore, we assessed the sensitivities of alveolar macrophages and alveolar epithelial cells to in vitro infection with BCG. First, alveolar macrophages were isolated from wild-type and $Lcn2^{-/-}$ mice, and infected with BCG (Fig. 5*A*). The CFU titers of BCG in macrophages at 4 and 7 days after infection were comparable between wild-type and $Lcn2^{-/-}$ cells. Thus, the absence of Lcn2 did not affect the anti-mycobacterial activity in alveolar macrophages. Next, we established AECs from wild-type and $Lcn2^{-/-}$ mice. Because AECs are difficult to culture in vitro, we took advantage of transgenic mice harboring a temperature-sensitive mutation of the SV40 large tumor Ag gene under the control of an IFN-γ-inducible H-$2K^b$ promoter element (30–32). Using these mice, we successfully established wild-type and $Lcn2^{-/-}$ AECs, both of which were stained with anti-SP-C Ab (data not shown). AECs from wild-type mice expressed Lcn2 mRNA and secreted Lcn2 protein into the culture medium when infected with BCG (data not shown). Thus, these AECs showed the characteristics of type II alveolar epithelial cells. AECs were infected with BCG, and the CFU titers within the cells were counted at 1, 2, 3, and 4 days after infection (Fig. 5*B*). At 3 and 4 days after infection, the CFU titers in $Lcn2^{-/-}$ cells were increased compared with those in wild-type cells. Addition of exogenous rLcn2 reduced the CFU numbers in $Lcn2^{-/-}$ cells (Fig. 5*C*). Taken together, these findings indicate that the high susceptibility of $Lcn2^{-/-}$ mice to *M. tuberculosis* infection is attributable to impaired clearance of mycobacteria from alveolar epithelial cells, rather than alveolar macrophages, in the absence of Lcn2.

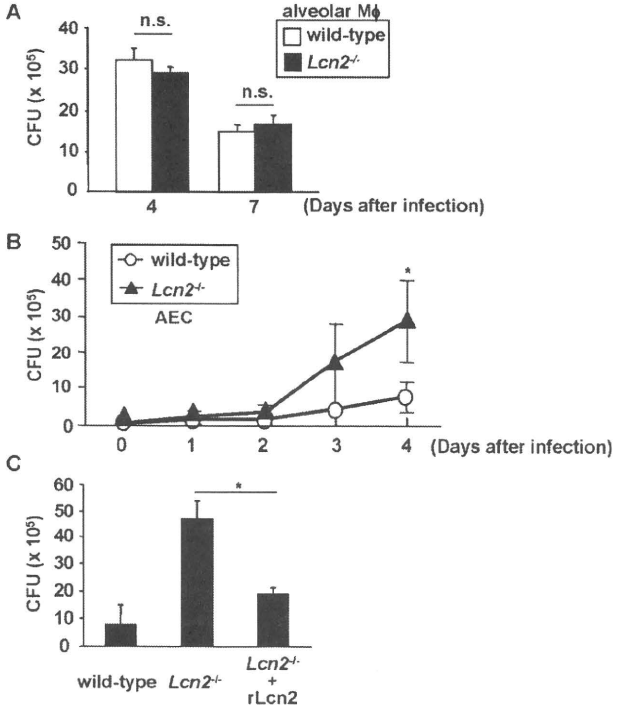

FIGURE 5. Increased BCG growth in $Lcn2^{-/-}$ alveolar epithelial cells. *A*, Alveolar macrophages were collected from uninfected wild-type and $Lcn2^{-/-}$ mice and cultured with BCG for the indicated periods. To eliminate external BCG, the cells were cultured with streptomycin for 1 h, washed three times, and harvested. Lysates of the cells were plated on 7H10-OADC agar, and the CFU numbers were counted. Representative data of two independent experiments are shown. n.s., not significant. *B*, Wild-type and $Lcn2^{-/-}$ AECs were cultured with BCG for the indicated periods. After removal of extracellular BCG, lysates the cells were plated on 7H10-OADC agar, and the CFU numbers were counted. Data are presented as means ± SD of triplicate determinations and are representative of three independent experiments. *, $p < 0.05$. Similar results were obtained when other AECs from wild-type and $Lcn2^{-/-}$ mice were used. *C*, Wild-type and $Lcn2^{-/-}$ AECs were cultured with BCG. At 2 days after infection, rLcn2 (final concentration 30 μg/ml) was added to the $Lcn2^{-/-}$ AEC. After an additional 2 days of culture, the cells were incubated with streptomycin for 1 h, washed three times, and harvested. Lysates of the cells were plated on 7H10-OADC agar, and the CFU numbers were counted. Representative data of three independent experiments are shown. Data are presented as means ± SD of triplicate determinations. *, $p < 0.05$.

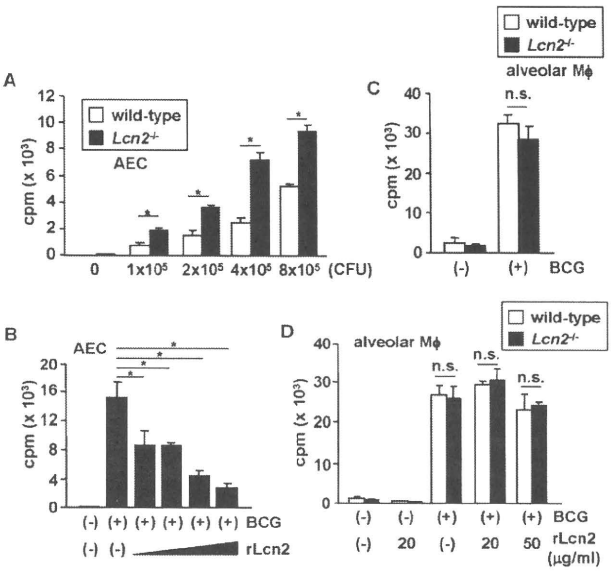

FIGURE 6. Lcn2-mediated inhibition of intracellular BCG growth. *A*, Wild-type and $Lcn2^{-/-}$ AECs were seeded onto 96-well plates and infected with the indicated CFUs of BCG for 6 h. The cells were then extensively washed to remove extracellular BCG and cultured in the presence of [^{3}H]uracil for 48 h. The incorporation of [^{3}H]uracil was measured. Data are presented as means ± SD of triplicate samples. Representative data of three independent experiments are shown. *, $p < 0.005$. *B*, $Lcn2^{-/-}$ AECs were seeded onto 96-well plates, and infected with BCG (2×10^5 CFU) for 6 h. After vigorous washing, the cells were cultured with increasing concentrations of rLcn2 (20, 30, 40, and 50 μg/ml) and [^{3}H]uracil for 48 h, before being measured for their [^{3}H]uracil incorporation. Data are presented as means ± SD of triplicate samples, and are representative of two independent experiments. * indicate a significant difference among groups, ANOVA, posthoc Scheffe, *, $p < 0.001$. *C*, Alveolar macrophages were collected from uninfected wild-type and $Lcn2^{-/-}$ mice, and cultured with BCG for 6 h. After vigorous washing, the cells were cultured in the presence of [^{3}H]uracil for 48 h, before being measured for their [^{3}H]uracil incorporation. Data are presented as the mean ± SD of triplicate samples. n.s., not significant. *D*, Alveolar macrophages from wild-type and $Lcn2^{-/-}$ mice were infected with BCG for 6 h. After vigorous washing, the cells were cultured in the presence of the indicated concentration of rLcn2 and [^{3}H]uracil for 48 h. Then, the [^{3}H]uracil incorporation was counted. Data are presented as means ± SD of triplicate samples. n.s., not significant.

Inhibition of intracellular mycobacterial growth by Lcn2

Mycobacteria are intracellular bacteria that replicate within cells. In the experiments performed so far, it is possible that extracellular growth was monitored as well as intracellular growth under the in vitro conditions. Therefore, to assess the intracellular growth of mycobacteria more precisely, we used [^{3}H]uracil, which is preferentially incorporated into mycobacterial nucleic acids (33). AECs derived from wild-type and $Lcn2^{-/-}$ mice were infected with several CFUs of BCG for 6 h, extensively washed with culture medium containing streptomycin to exclude extracellular BCG, and then cultured for 2 days in the presence of [^{3}H]uracil (Fig. 6*A*). Under these conditions, [^{3}H]uracil incorporation was below 1×10^2 cpm in wells containing uninfected AECs or wells placed in contact with BCG and then extensively washed. After infection with each CFU, [^{3}H]uracil incorporation was increased in $Lcn2^{-/-}$ cells compared with wild-type cells. In BCG-infected $Lcn2^{-/-}$ cells, addition of exogenous rLcn2 reduced the uptake of [^{3}H]uracil by intracellular BCG (Fig. 6*B*). In alveolar macrophages, the [^{3}H]uracil incorporation by intracellular BCG was comparable between wild-type and $Lcn2^{-/-}$ cells (Fig. 6*C*). Addition of rLcn2 did not effectively reduce the uptake of [^{3}H]uracil by intracellular BCG in alveolar macrophages from both wild-type and $Lcn2^{-/-}$ mice (Fig. 6*D*). These findings indicate that extracellular Lcn2 limits intracellular growth of BCG in AECs, but not in alveolar macrophages.

Because extracellular Lcn2 modulated intracellular mycobacterial growth in the AECs, we analyzed whether extracellular Lcn2 was incorporated into the AECs as described in several previous reports (18, 19). AECs were infected with GFP-expressing BCG and then treated with fluorescein-labeled rLcn2 (Fig. 7*A*). Lcn2 was detected within the AECs, and colocalized with dextran that was taken up into the cells by endocytosis. Furthermore, many BCG were colocalized with rLcn2, indicating that endocytosed Lcn2 was in close proximity to intracellular BCG. In contrast, although Lcn2 was incorporated into alveolar macrophages, the incorporated Lcn2 was not colocalized with BCG in alveolar macrophages (Fig. 7*B*), indicating that BCG and rLcn2 were localized in distinct cellular compartments within macrophages. We blocked

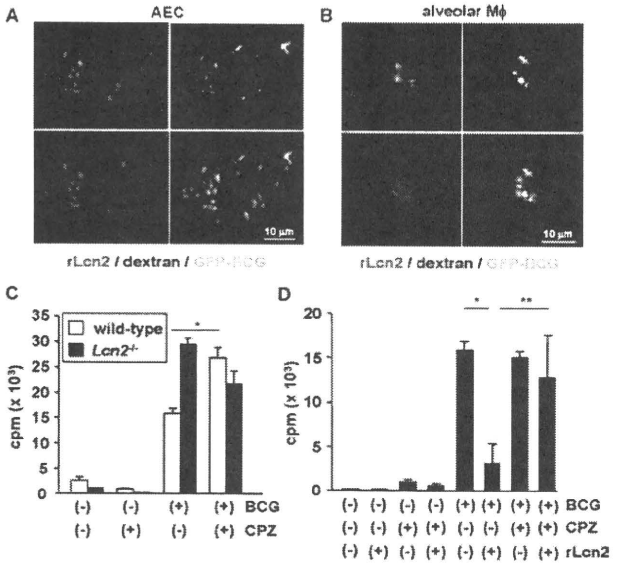

FIGURE 7. Requirement of Lcn2 incorporation for the inhibition of intracellular BCG growth. *A*, GFP-expressing BCG (green)-infected alveolar epithelial cells were cultured with dextran (25 μg/ml; blue) and fluorescein-labeled rLcn2 (15 μg/ml; red) for 6 h. The cells were then washed, fixed with 4% PFA, and analyzed by confocal microscopy. Data are representative of three independent experiments. *B*, GFP-expressing BCG (green)-infected alveolar macrophages were cultured with dextran (25 μg/ml; blue) and fluorescein-labeled rLcn2 (15 μg/ml; red) for 6 h. The cells were then washed, fixed with 4% PFA for 5 min, and analyzed by confocal microscopy. *C*, Wild-type and $Lcn2^{-/-}$ AECs were seeded onto 96-well plates and infected with BCG (2×10^5 CFU) for 6 h. After extensive washing, the cells were cultured with CPZ (10 μM) and [^{3}H]uracil for 48 h. The [^{3}H]uracil incorporation was then measured. Data are presented as means ± SD of triplicate samples, and are representative of two independent experiments. *, $p < 0.01$. *D*, $Lcn2^{-/-}$ AECs were seeded onto 96-well plates, and infected with BCG for 6 h. After washing, the cells were cultured with CPZ for 30 min and then cultured with rLcn2 (20 μg/ml) and [^{3}H]uracil for 48 h. The [^{3}H]uracil incorporation was measured. Data are presented as means ± SD of triplicate samples, and are representative of two independent experiments. * or ** indicate a significant difference among groups, ANOVA, posthoc Scheffe, *, $p < 0.005$; **, $p < 0.05$.

endocytosis of Lcn2 using CPZ after BCG infection. Addition of CPZ resulted in increased BCG growth in wild-type AECs, but not in $Lcn2^{-/-}$ cells (Fig. 7*C*). We also analyzed the effects of the endocytosis inhibitor on rLcn2-mediated inhibition of BCG growth (Fig. 7*D*). Addition of CPZ abolished Lcn2-mediated inhibition of [^{3}H]uracil incorporation in both wild-type and $Lcn2^{-/-}$ cells. Cytochalasin B, which also blocks endocytosis, had similar effects to those of CPZ on Lcn2-mediated inhibition of intracellular BCG growth (data not shown). These findings indicate that endocytosed Lcn2 inhibits the intracellular growth of BCG in AECs.

Discussion

Lcn2 has a variety of putative functions, as evident from its many different names such as neutrophil gelatinase-associated lipocalin, uterocalin, 24p3, and siderocalin (12, 13, 16, 19). In the context of its function in host defense, a structural study of the Lcn2 protein revealed that it associates with enterobactin-type bacterial siderophores (16). Subsequently, Lcn2 was shown to bind to several types of siderophores such as caroboxy-mycobactin and bacillibactin (20, 21). In addition, Lcn2 has been proposed to bind to an as-yet unknown mammalian siderophore (18, 34). Thus, Lcn2 has the ability to bind to a variety of types of siderophores. Furthermore, Lcn2 has been shown to inhibit the growth of *E. coli* through sequestration of iron uptake (22, 23). The present study has demonstrated that Lcn2 also participates in the inhibition of mycobacterial growth through similar mechanisms to those against *E. coli*. Indeed, Lcn2 has been shown to associate with the mycobacteria-derived hydrophilic siderophore carboxy-mycobactin (21). In accordance with our results, Lcn2 has been shown to be secreted from neutrophils during *M. tuberculosis* infection and inhibit their growth (35). Lcn2 was originally identified as a molecule that is secreted from neutrophils, which are rapidly recruited to *M. tuberculosis*-infected lungs. Therefore, neutrophils are presumably the source of Lcn2 as well as alveolar macrophages and epithelial cell during *M. tuberculosis* infection.

Regarding the high sensitivity of $Lcn2^{-/-}$ mice to *M. tuberculosis* infection, it is noteworthy that $Lcn2^{-/-}$ alveolar epithelial cells, but not macrophages, contained increased numbers of *M. tuberculosis* at the early phase of the infection, as evaluated by histopathological and immunohistochemical analyses. This finding was unexpected, because successful in vivo detection of mycobacteria in respiratory epithelial cells in wild-type mice has only been achieved through analyses of mycobacterial DNA or use of electron microscopy, even though mycobacteria have been shown to invade epithelial cells as well as macrophages in vitro (6–9, 36). In addition, $Lcn2^{-/-}$ alveolar epithelial cells, but not macrophages, exhibited defective inhibition of intracellular mycobacterial growth, suggesting that impaired inhibition of mycobacterial growth in alveolar epithelial cells due to the absence of Lcn2 may be a major cause of the high susceptibility $Lcn2^{-/-}$ mice to *M. tuberculosis* infection. Given that mycobacteria were easily detected in the alveolar epithelial cell layers by a typical histological approach in the absence of Lcn2 and the increased mycobacterial growth was observed in $Lcn2^{-/-}$ epithelial cells, but not in macrophages, epithelial cells may play an important role in the host immune responses against respiratory infection with *M. tuberculosis*.

Mycobacteria replicate within cells in vivo, and several lines of evidence indicate that mycobactin-mediated iron uptake is a prerequisite for intracellular mycobacterial growth (27, 29). Consistent with previous studies (18, 19), our findings indicated that Lcn2 is internalized into alveolar epithelial cells via endocytosis. Furthermore, addition of rLcn2 effectively inhibited intracellular mycobacterial growth in AECs, and this effect was abolished by endocytosis inhibitors. At present, it remains unclear how mycobacteria take up iron within epithelial cells using mycobactin. First, it is apparent that mycobacteria exist in the phagosome of macrophages. However, the subcellular localization of mycobacteria within epithelial cells has not been established, although mycobacteria have been shown to be localized in endosomes or macropinosomes (37, 38). Our results revealed colocalization of mycobacteria and dextran, indicating that mycobacteria exist in the endosome-like vacuole within epithelial cells. Second, it remains obscure whether mycobacteria secrete water-soluble carboxy-mycobactin into the cytoplasm to bind the cytosolic iron. It is also obscure how endocytosed Lcn2 approaches the carboxy-mycobactin/iron complexes within the cells. Given that Lcn2 and mycobacteria are colocalized within the endosome-like structure, it is possible that mycobacteria take up the iron entering the endosome using mycobactin, and endocytosed Lcn2, in turn, binds to the carboxy-mycobactin/iron complexes, thereby blocking iron acquisition by mycobacteria. Further studies are required to clarify the precise mechanisms for the interaction between Lcn2 and mycobacteria-derived carboxy-mycobactin.

In alveolar macrophages, the absence of Lcn2 did not affect the sensitivity to mycobacterial infection. This may be due to the differential localizations of mycobacteria in epithelial cells and macrophages. Lcn2 was colocalized with mycobacteria in epithelial

cells, indicating that mycobacteria exist within the endosome-like structure. In contrast, mycobacteria were localized within the phagosome in macrophages, leading to distinct localizations of Lcn2 and mycobacteria in macrophages. Alternatively, macrophages are professional cells that kill intracellular bacteria by producing several macrophage-specific anti-microbial mediators, including NO synthase and Nramp1 (39–41). These mediators may compensate the Lcn2 deficiency in macrophages. In contrast, they are not expressed in epithelial cells, resulting in the high sensitivity to mycobacterial infection in the absence of Lcn2. Thus, in alveolar epithelial cells, Lcn2 may be a major factor that mediates host resistance to mycobacterial infection.

Our results highlight a novel innate host defense system that inhibits mycobacterial infection at the respiratory mucosal surface. We would like to propose the following scenario with regard to the function of Lcn2. Lcn2 is secreted into the alveolar space by alveolar macrophages and epithelial cells during the early phase of respiratory mycobacterial infection. Lcn2 presumably inhibits mycobacterial growth within the alveolar space. In addition, Lcn2 is internalized into the alveolar epithelial cells, which are invaded by mycobacteria, and inhibits mycobacterial growth by sequestering iron uptake. This leads to a reduction in the number of infected mycobacteria at the early phase of infection, which may help to create sufficient time for effective activation of anti-mycobacterial innate and adaptive immune responses. Thus, respiratory epithelial cells play an active role in the resistance to mycobacterial infection, in addition to their functions as physical barriers and secretors of anti-bacterial mediators.

Acknowledgments

We thank I. Sugawara for providing the *M. tuberculosis* H37Rv, Y. Yamada and K. Takeda for technical assistance, and M. Kurata and M. Yasuda for secretarial assistance.

Disclosures

The authors have no financial conflict of interest.

References

1. North, R. J., and Y. J. Jung. 2004. Immunity to tuberculosis. *Annu. Rev. Immunol.* 22: 599–623.
2. Kaufmann, S. H. 2006. Tuberculosis: back on the immunologists' agenda. *Immunity* 24: 351–357.
3. Quesniaux, V., C. Fremond, M. Jacobs, S. Parida, D. Nicolle, V. Yeremeev, F. Bihl, F. Erard, T. Botha, M. Drennan, et al. 2004. Toll-like receptor pathways in the immune responses to mycobacteria. *Microbes Infect.* 6: 946–959.
4. Fremond, C. M., V. Yeremeev, D. M. Nicolle, M. Jacobs, V. F. Quesniaux, and B. Ryffel. 2004. Fatal *Mycobacterium tuberculosis* infection despite adaptive immune response in the absence of MyD88. *J. Clin. Invest.* 114: 1790–1799.
5. Aoki, K., S. Matsumoto, Y. Hirayama, T. Wada, Y. Ozeki, M. Niki, P. Domenech, K. Umemori, S. Yamamoto, A. Mineda, et al. 2004. Extracellular mycobacterial DNA-binding protein 1 participates in mycobacterium-lung epithelial cell interaction through hyaluronic acid. *J. Biol. Chem.* 279: 39798–39806.
6. Teitelbaum, R., W. Schubert, L. Gunther, Y. Kress, F. Macaluso, J. W. Pollard, D. N. McMurray, and B. R. Bloom. 1999. The M cell as a portal of entry to the lung for the bacterial pathogen *Mycobacterium tuberculosis*. *Immunity* 10: 641–651.
7. Bermudez, L. E., and F. J. Sangari. 2001. Cellular and molecular mechanisms of internalization of mycobacteria by host cells. *Microbes Infect.* 3: 37–42.
8. Bermudez, L. E., F. J. Sangari, P. Kolonoski, M. Petrofsky, and J. Goodman. 2002. The efficiency of the translocation of *Mycobacterium tuberculosis* across a bilayer of epithelial and endothelial cells as a model of the alveolar wall is a consequence of transport within mononuclear phagocytes and invasion of alveolar epithelial cells. *Infect. Immun.* 70: 140–146.
9. Hernandez-Pando, R., M. Jeyanathan, G. Mengistu, D. Aguilar, H. Orozco, M. Harboe, G. A. Rook, and G. Bjune. 2000. Persistence of DNA from *Mycobacterium tuberculosis* in superficially normal lung tissue during latent infection. *Lancet* 356: 2133–2138.
10. Ferguson, J. S., and L. S. Schlesinger. 2000. Pulmonary surfactant in innate immunity and the pathogenesis of tuberculosis. *Tuber. Lung Dis.* 80: 173–184.
11. Kjeldsen, L., J. B. Cowland, and N. Borregaard. 2000. Human neutrophil gelatinase-associated lipocalin and homologous proteins in rat and mouse. *Biochim. Biophys. Acta* 1482: 272–283.
12. Devireddy, L. R., J. G. Teodoro, F. A. Richard, and M. R. Green. 2001. Induction of apoptosis by a secreted lipocalin that is transcriptionally regulated by IL-3 deprivation. *Science* 293: 829–834.
13. Kjeldsen, L., A. H. Johnsen, H. Sengelov, and N. Borregaard. 1993. Isolation and primary structure of NGAL, a novel protein associated with human neutrophil gelatinase. *J. Biol. Chem.* 268: 10425–10432.
14. Flower, D. R., A. C. North, and T. K. Attwood. 1991. Mouse oncogene protein 24p3 is a member of the lipocalin protein family. *Biochem. Biophys. Res. Commun.* 180: 69–74.
15. Liu, Q., J. Ryon, and M. Nilsen-Hamilton. 1997. Uterocalin: a mouse acute phase protein expressed in the uterus around birth. *Mol. Reprod. Dev.* 46: 507–514.
16. Goetz, D. H., M. A. Holmes, N. Borregaard, M. E. Bluhm, K. N. Raymond, and R. K. Strong. 2002. The neutrophil lipocalin NGAL is a bacteriostatic agent that interferes with siderophore-mediated iron acquisition. *Mol. Cell* 10: 1033–1043.
17. Nilsen-Hamilton, M., Q. Liu, J. Ryon, L. Bendickson, P. Lepont, and Q. Chang. 2003. Tissue involution and the acute phase response. *Ann. NY Acad. Sci.* 995: 94–108.
18. Devireddy, L. R., C. Gazin, X. Zhu, and M. R. Green. 2005. A cell-surface receptor for lipocalin 24p3 selectively mediates apoptosis and iron uptake. *Cell* 123: 1293–1305.
19. Yang, J., D. Goetz, J. Y. Li, W. Wang, K. Mori, D. Setlik, T. Du, H. Erdjument-Bromage, P. Tempst, R. Strong, and J. Barasch. 2002. An iron delivery pathway mediated by a lipocalin. *Mol. Cell* 10: 1045–1056.
20. Abergel, R. J., M. K. Wilson, J. E. Arceneaux, T. M. Hoette, R. K. Strong, B. R. Byers, and K. N. Raymond. 2006. Anthrax pathogen evades the mammalian immune system through stealth siderophore production. *Proc. Natl. Acad. Sci. USA* 103: 18499–18503.
21. Holmes, M. A., W. Paulsene, X. Jide, C. Ratledge, and R. K. Strong. 2005. Siderocalin (Lcn 2) also binds carboxymycobactins, potentially defending against mycobacterial infections through iron sequestration. *Structure* 13: 29–41.
22. Flo, T. H., K. D. Smith, S. Sato, D. J. Rodriguez, M. A. Holmes, R. K. Strong, S. Akira, and A. Aderem. 2004. Lipocalin 2 mediates an innate immune response to bacterial infection by sequestrating iron. *Nature* 432: 917–921.
23. Berger, T., A. Togawa, G. S. Duncan, A. J. Elia, A. You-Ten, A. Wakeham, H. E. Fong, C. C. Cheung, and T. W. Mak. 2006. Lipocalin 2-deficient mice exhibit increased sensitivity to *Escherichia coli* infection but not to ischemia-reperfusion injury. *Proc. Natl. Acad. Sci. USA* 103: 1834–1839.
24. Smith, K. D. 2007. Iron metabolism at the host pathogen interface: lipocalin 2 and the pathogen-associated iroA gene cluster. *Int. J. Biochem. Cell Biol.* 39: 1776–1780.
25. Houben, E. N., L. Nguyen, and J. Pieters. 2006. Interaction of pathogenic mycobacteria with the host immune system. *Curr. Opin. Microbiol.* 9: 76–85.
26. De Voss, J. J., K. Rutter, B. G. Schroeder, and C. E. Barry, 3rd. 1999. Iron acquisition and metabolism by mycobacteria. *J. Bacteriol.* 181: 4443–4451.
27. De Voss, J. J., K. Rutter, B. G. Schroeder, H. Su, Y. Zhu, and C. E. Barry, 3rd. 2000. The salicylate-derived mycobactin siderophores of *Mycobacterium tuberculosis* are essential for growth in macrophages. *Proc. Natl. Acad. Sci. USA* 97: 1252–1257.
28. Gobin, J., and M. A. Horwitz. 1996. Exochelins of *Mycobacterium tuberculosis* remove iron from human iron-binding proteins and donate iron to mycobactins in the *M. tuberculosis* cell wall. *J. Exp. Med.* 183: 1527–1532.
29. Luo, M., E. A. Fadeev, and J. T. Groves. 2005. Mycobactin-mediated iron acquisition within macrophages. *Nat. Chem. Biol.* 1: 149–153.
30. Jat, P. S., M. D. Noble, P. Ataliotis, Y. Tanaka, N. Yannoutsos, L. Larsen, and D. Kioussis. 1991. Direct derivation of conditionally immortal cell lines from an H-2Kb-tsA58 transgenic mouse. *Proc. Natl. Acad. Sci. USA* 88: 5096–5100.
31. Whitehead, R. H., P. E. VanEeden, M. D. Noble, P. Ataliotis, and P. S. Jat. 1993. Establishment of conditionally immortalized epithelial cell lines from both colon and small intestine of adult H-2Kb-tsA58 transgenic mice. *Proc. Natl. Acad. Sci. USA* 90: 587–591.
32. deMello, D. E., S. Mahmoud, P. J. Padfield, and J. W. Hoffmann. 2000. Generation of an immortal differentiated lung type-II epithelial cell line from the adult H-2K(b)tsA58 transgenic mouse. *In Vitro Cell. Dev. Biol. Anim.* 36: 374–382.
33. Rook, G. A., B. R. Champion, J. Steele, A. M. Varey, and J. L. Stanford. 1985. I-A restricted activation by T cell lines of anti-tuberculosis activity in murine macrophages. *Clin. Exp. Immunol.* 59: 414–420.
34. Mori, K., H. T. Lee, D. Rapoport, I. R. Drexler, K. Foster, J. Yang, K. M. Schmidt-Ott, X. Chen, J. Y. Li, S. Weiss, et al. 2005. Endocytic delivery of lipocalin-siderophore-iron complex rescues the kidney from ischemia-reperfusion injury. *J. Clin. Invest.* 115: 610–621.
35. Martineau, A. R., S. M. Newton, K. A. Wilkinson, B. Kampmann, B. M. Hall, N. Nawroly, G. E. Packe, R. N. Davidson, C. J. Griffiths, and R. J. Wilkinson. 2007. Neutrophil-mediated innate immune resistance to mycobacteria. *J. Clin. Invest.* 117: 1988–1994.
36. Sato, K., H. Tomioka, T. Shimizu, T. Gonda, F. Ota, and C. Sano. 2002. Type II alveolar cells play roles in macrophage-mediated host innate resistance to pulmonary mycobacterial infections by producing proinflammatory cytokines. *J. Infect. Dis.* 185: 1139–1147.
37. Bermudez, L. E., and J. Goodman. 1996. *Mycobacterium tuberculosis* invades and replicates within type II alveolar cells. *Infect. Immun.* 64: 1400–1406.
38. Garcia-Perez, B. E., R. Mondragon-Flores, and J. Luna-Herrera. 2003. Internalization of *Mycobacterium tuberculosis* by macropinocytosis in non-phagocytic cells. *Microb. Pathog.* 35: 49–55.
39. Adams, D. O., and T. A. Hamilton. 1984. The cell biology of macrophage activation. *Annu. Rev. Immunol.* 2: 283–318.
40. MacMicking, J., Q. W. Xie, and C. Nathan. 1997. Nitric oxide and macrophage function. *Annu. Rev. Immunol.* 15: 323–350.
41. Govoni, G., and P. Gros. 1998. Macrophage NRAMP1 and its role in resistance to microbial infections. *Inflamm. Res.* 47: 277–284.

Potent Antimycobacterial Activity of Mouse Secretory Leukocyte Protease Inhibitor[1]

Junichi Nishimura,*§ Hiroyuki Saiga,*‡ Shintaro Sato,¶ Megumi Okuyama,‖ Hisako Kayama,*‡ Hirotaka Kuwata,* Sohkichi Matsumoto,‖ Toshirou Nishida,§ Yoshiki Sawa,§ Shizuo Akira,¶ Yasunobu Yoshikai,† Masahiro Yamamoto,‡ and Kiyoshi Takeda[2]*‡

Secretory leukocyte protease inhibitor (SLPI) has multiple functions, including inhibition of protease activity, microbial growth, and inflammatory responses. In this study, we demonstrate that mouse SLPI is critically involved in innate host defense against pulmonary mycobacterial infection. During the early phase of respiratory infection with *Mycobacterium bovis* bacillus Calmette-Guérin, SLPI was produced by bronchial and alveolar epithelial cells, as well as alveolar macrophages, and secreted into the alveolar space. Recombinant mouse SLPI effectively inhibited in vitro growth of bacillus Calmette-Guérin and *Mycobacterium tuberculosis* through disruption of the mycobacterial cell wall structure. Each of the two whey acidic protein domains in SLPI was sufficient for inhibiting mycobacterial growth. Cationic residues within the whey acidic protein domains of SLPI were essential for disruption of mycobacterial cell walls. Mice lacking SLPI were highly susceptible to pulmonary infection with *M. tuberculosis*. Thus, mouse SLPI is an essential component of innate host defense against mycobacteria at the respiratory mucosal surface. *The Journal of Immunology*, 2008, 180: 4032–4039.

Mycobacterium tuberculosis is a top killer among bacterial pathogens and is responsible for 2 million deaths annually. The emergence of AIDS and development of multidrug-resistant *M. tuberculosis* have increased the incidence of tuberculosis, and it has now become a serious problem. Therefore, the host defense mechanisms against *M. tuberculosis* have been intensively investigated and important roles of T cell-mediated adaptive immunity are now well established (1, 2). In addition, functional characterization of TLRs has recently indicated the importance of innate immunity in infection with *M. tuberculosis* (3, 4). Macrophages and dendritic cells are the major effectors of TLR-mediated antimycobacterial immune responses, because they produce a variety of proinflammatory cytokines and have the capacity of phagocytosis. However, during *M. tuberculosis* infection, epithelial cells in the respiratory tract as well as alveolar macrophages are the first targets for invasion by *M. tuberculosis*. Therefore, these epithelial cells are expected to play roles in preventing mycobacterial infection by establishing physical barriers and producing proinflammatory and antimicrobial mediators (5).

Secretory leukocyte protease inhibitor (SLPI)[3] is a 12-kDa secreted protein composed of two cysteine-rich whey acidic protein (WAP) domains (also called WAP four-disulfide core (WFDC) domains) (6–8). It was originally identified in seminal fluid and is produced by secretory cells in the genital, respiratory, and lacrimal glands as well as dermal keratinocytes (9–13). SLPI is a potent inhibitor of serine proteases, such as neutrophil elastase and cathepsin G, and has therefore been proposed to protect tissues from protease-mediated damage at sites of inflammation (14, 15). Indeed, SLPI was subsequently shown to mediate wound healing (16, 17). Further studies have revealed that SLPI has additional functions. For example, it possesses an antimicrobial activities against Gram-negative and Gram-positive bacteria, fungi, and viruses, including HIV (18–20). In addition to SLPI, several other serine protease inhibitors containing a single WAP domain, such as Eppin, Elafin, SWAM1, and SWAM2, also possess antimicrobial activities against Gram-negative and Gram-positive bacteria (8, 21, 22). Thus, serine protease inhibitors possessing WAP domains exhibit antimicrobial activities. However, the precise mechanisms by which these serine protease inhibitors exert their antimicrobial activities remain elusive. More recently, SLPI was found to mediate anti-inflammatory responses. Briefly, SLPI is induced in monocytes and macrophages in response to inflammatory stimuli mediated by TLRs (23) and subsequently suppresses TLR-dependent production of inflammatory mediators in macrophages by modulating NF-κB activity (23–25). Consistent with these findings, SLPI-deficient mice are highly sensitive to TLR4 ligand (LPS)-induced endotoxin shock with increased production of IL-6 (26). Thus, SLPI has diverse functions and its precise roles need to be investigated more carefully.

*Deparment of Molecular Genetics and †Division of Host Defense, Research Center for Prevention of Infectious Diseases, Medical Institute of Bioregulation, Kyushu University, Fukuoka; ‡Laboratory of Immune Regulation, Department of Microbiology and Immunology, §Department of Surgery, Graduate School of Medicine, and ¶Department of Host Defense, Research Institute for Microbial Diseases, Osaka University; and ‖Department of Host Defense, Osaka City University Graduate School of Medicine, Osaka, Japan

Received for publication April 3, 2007. Accepted for publication January 9, 2008.

The costs of publication of this article were defrayed in part by the payment of page charges. This article must therefore be hereby marked *advertisement* in accordance with 18 U.S.C. Section 1734 solely to indicate this fact.

[1] This work was supported by a Grant-in-Aid from the Ministry of Education, Culture, Sports, Science and Technology and the Ministry of Health, Labor and Welfare, as well as the Tokyo Biochemical Research Foundation, the Cell Science Research Foundation, the Yakult Bio-Science Foundation, the Osaka Foundation for Promotion of Clinical Immunology, the Sumitomo Foundation, and the Sankyo Foundation of Life Science.

[2] Address correspondence and reprint requests to Dr. Kiyoshi Takeda, Laboratory of Immune Regulation, Department of Microbiology and Immunology, Graduate School of Medicine, Osaka University, Suita, Osaka, 565-0871, Japan. E-mail address: ktakeda@ongene.med.osaka-u.ac.jp

[3] Abbreviations used in this paper: SLPI, secretory leukocyte protease inhibitor; WAP, whey acidic protein; WFDC, WAP four-disulfide core; qPCR, quantitative PCR; BALF, bronchoalveolar lavage fluid; BCG, bacillus Calmette-Guérin; FLUOS, 5-(6-)carboxyfluorescein-*N*-hydroxysuccinimide ester; NPN, 1-*N*-phenylnapthylamine; AEC, alveolar epithelial cell.

Copyright © 2008 by The American Association of Immunologists, Inc. 0022-1767/08/$2.00

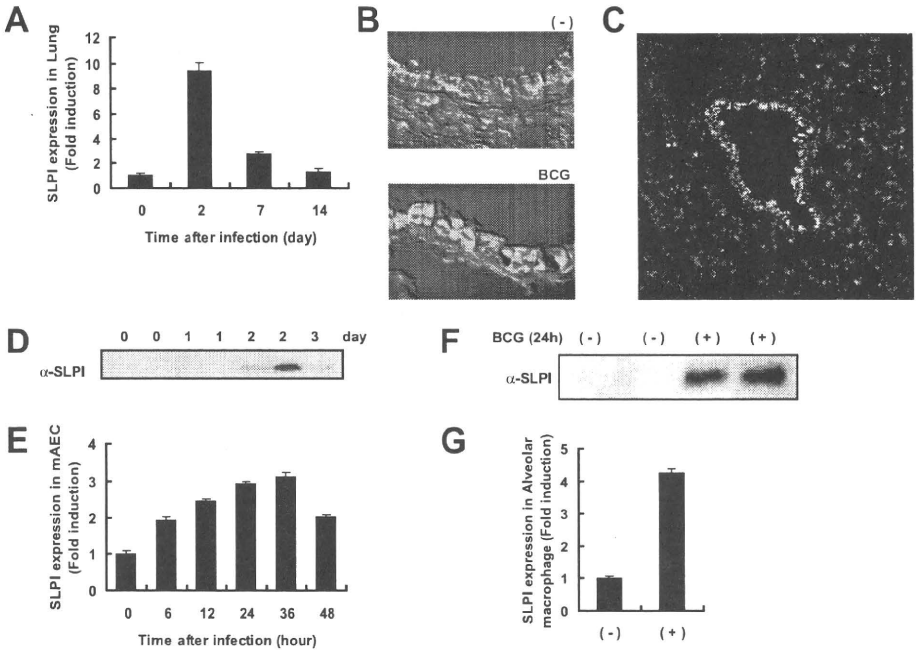

FIGURE 1. Expression of SLPI during mycobacterium infection. *A*, Wild-type mice were intratracheally infected with BCG (4×10^5 CFU). At the indicated periods, total RNA was extracted from the lungs. SLPI mRNA expression was analyzed by quantitative real-time RT-PCR. Data are shown as the relative mRNA levels normalized by the corresponding 18S rRNA level. *B* and *C*, At 2 days after intratracheal infection with BCG, lung tissue sections were stained with an anti-SLPI Ab (red) and 4′,6-diamidino-2-phenylindole (blue) and visualized by fluorescence microscopy. *D*, BALF was collected at the indicated periods after BCG infection. Mouse SLPI protein expression was analyzed by Western blotting with an anti-SLPI Ab. Data obtained from two independent mice (0, 1, and 2 days) are indicated. *E*, AEC were incubated with the same number of BCG for the indicated periods. SLPI mRNA expression was analyzed by quantitative real-time RT-PCR. Data are shown as the relative mRNA levels normalized by the corresponding 18S rRNA level. *F*, AEC were incubated with the same number of BCG. Culture supernatants were collected before (−) and after 24 h of infection (+) and subjected to Western blot analysis using an anti-SLPI Ab. Data obtained from two independent cell clones are shown. *G*, Alveolar macrophages were collected from uninfected wild-type mice, cultured with or without BCG for 48 h, and then analyzed for their SLPI mRNA expression by quantitative real-time RT-PCR. The results are presented as the mean ± SD.

In this study, we investigated the roles of murine SLPI in the context of host defenses against mycobacteria, since SLPI expression is greatly induced in macrophages and the lungs during mycobacterial infection (27). Recombinant SLPI inhibited mycobacterial growth at a lower concentration than that required to inhibit bacterial growth. Inhibition of mycobacterial growth was mediated by increased permeability of the mycobacterial membrane. Mutation of cationic residues in the WAP domains of SLPI resulted in loss of its antimycobacterial activity. Furthermore, SLPI-deficient mice were highly susceptible to pulmonary infection with *M. tuberculosis*. These findings demonstrate that SLPI is a potent antimycobacterial molecule.

Materials and Methods

Cells and bacteria

M. tuberculosis strains H37Ra (ATCC 25177; American Type Culture Collection) and *M. tuberculosis* strains H37Rv (28) were grown in Middlebrook 7H9-ADC medium for 2 wk and stored at −80°C until use. *Mycobacterium bovis* bacillus Calmette-Guérin (BCG; Tokyo strain) was purchased from Kyowa Pharmaceuticals. *Salmonella enterica* serovar *typhimurium* were provided by the Research Institute for Microbial Diseases (Osaka University). For each experiment, the dose was confirmed by plating an aliquot of the injected bacterial suspension. Isolation and immortalization of type II alveolar epithelial cells from the lungs of transgenic H-2K^b-tsA58 mice were performed as previously described (29), with some modifications.

Immunohistochemistry

Lungs were washed with PBS and frozen in Tissue-Tex OCT compound (Sakura, Tokyo, Japan). Cryostat sections (5-μm thick) were fixed with cold acetone for 10 min, dried, rehydrated with PBS, and blocked with PBS containing 20 mM HEPES, 10% FBS, and 1 μg of Fc-blocking mAb (2.4G2; BD Pharmingen). Next, the sections were sequentially incubated with a biotinylated anti-mouse SLPI Ab (R&D Systems) and Alexa Fluor 594-conjugated streptavidin (Molecular Probes). The nuclei were stained with 4′,6-diamidino-2-phenylindole (Molecular Probes). After washing with PBS, the sections were analyzed by confocal microscopy (Zeiss).

Western blot analysis

Samples were boiled for 5 min in reducing SDS-PAGE sample buffer and then subjected to SDS-PAGE. The separated proteins were transferred to a 0.45-μm pore polyvinylidene fluoride membrane (Millipore). After blocking with 5% milk, the membrane was incubated with the above-described biotinylated anti-mouse SLPI Ab (0.2 μg/ml) and a streptavidin-HRP complex (1/10,000 dilution; R&D Systems). The bound Abs were detected by the Super Signal reagent (Pierce).

Quantitative real-time RT-PCR

After isolation of total RNA with the TRIzol reagent (Invitrogen Life Technologies), 4 μg of the RNA was treated with RQ1DNase (Promega) and then reverse-transcribed using Moloney murine leukemia virus reverse transcriptase (Promega) and Random Primers (Toyobo). Gene expression was quantified with an Applied Biosystems PRISM 7000 sequence detection system using TaqMan Universal PCR Master Mix (Applied Biosystems). To determine the relative expression level of each sample, the corresponding 18S rRNA expression level was measured as an internal control. The primer and probe sequences for SLPI were follows: quantitative PCR (qPCR) primer (forward), 5′-d(GCTGTGAGGGTATATGTG GGAAA)-3′; qPCR primer (reverse), 5′-d(CGCCAATGTCAGGGAT CAG)-3′; and qPCR probe, 5′-FAMd(TCTGCCTGCCCCCGATGTG AG)BHQ-3′.